Imaging of the Renal Transplant Recipient

32

Maria Manning and Jade Wong-You-Cheong

Ultrasound

Ultrasound (US) is the most frequently used imaging technique in renal transplantation. The superficial location of the renal transplant in the iliac fossa allows access for high-resolution ultrasound imaging. Gray scale evaluation of renal transplant morphology includes evaluation of the size, corticomedullary differentiation, and echotexture of the allograft, as well as detection of hydronephrosis, stone or mass, and postoperative complications such as fluid collections or hematomas. Morphologically, the transplanted kidney has similar imaging characteristics as the native kidney (Fig. 32.1a), though corticomedullary differentiation and vasculature are better seen in most patients. Once transplanted, there is compensatory hypertrophy of the allograft, which grows by approximately 40 % within 6 months following transplantation [1]. The collecting system of the normal transplant may be mildly dilated due to increased volume of urine produced by the sole functioning kidney and possibly due to minor reflux at the ureterovesical anastomosis [2]. The bladder is also evaluated.

Morphologic evaluation is supplemented by color/power and duplex Doppler evaluation for parenchymal blood flow and patency of the renal arteries (single or multiple) and veins (Fig. 32.1b–d). Doppler ultrasound is an ideal initial modality for the detection and evaluation of vascular complications such as thrombosis, stenosis, or arteriovenous fistulae. Pediatric en bloc transplants are technically more challenging because of the smaller size of the renal arteries and veins (Fig. 32.2a, b). Normal Doppler arterial waveforms consist of continuous antegrade flow throughout the cardiac cycle with low resistance diastolic flow (Fig. 32.3). Abnormal intrarenal arterial resistance can be quantified by calculation of indices such as the resistive index (RI) and the pulsatility index (Fig. 32.3). While both indices reflect altered hemodynamics, the resistive index (RI) is the most commonly used. Normal resistive index ranges from 0.65 to 0.70 [3, 4]. RI values depend on local vascular status rather than renal function, and measurements are neither very sensitive nor specific [5, 6]. Causes of increased intrarenal resistive index include rejection, acute tubular necrosis (ATN), hydronephrosis, and vascular thrombosis. Though nonspecific for diagnosis, elevated RI values after transplantation have been shown to be associated with poor allograft and patient survival [7].

Research is ongoing in the evaluation of contrast-enhanced ultrasound using microbubble contrast agents, which is performed regularly outside of the United States, and has shown promise in the evaluation of renal transplant perfusion [8], specifically as a potential noninvasive means in the differentiation of acute rejection versus ATN as the cause of delayed graft function [9]. However, at this time, ultrasound cannot distinguish the causes of graft dysfunction, and biopsy remains the standard for diagnosis.

Ultrasound is a real-time, rapidly performed modality that is widely available and relatively cheap. It can be performed at the bedside, as is often required, and does not use ionizing radiation or nephrotoxic contrast. Limitations include suboptimal visualization in patients with large body habitus and extensive intestinal gas. Additionally, the quality of ultrasound examinations is dependent upon the technical skills and experience of the operator. Ultrasound is highly sensitive in the detection of hydronephrosis, fluid collections, and vascular complications. It is also an excellent modality for guidance during interventional procedures, such as biopsy (Fig. 32.4), aspiration or drainage of fluid collections, and access for antegrade pyelography or percutaneous nephrostomy placement.

M. Manning, M.D. • J. Wong-You-Cheong, M.D. (✉)
Department of Diagnostic Radiology, University of Maryland School of Medicine, 22 S. Greene Street, Baltimore, MD 21201-1595, USA
e-mail: MManning@umm.edu; JWong@umm.edu

M.R. Weir and E.V. Lerma (eds.), *Kidney Transplantation: Practical Guide to Management*,
DOI 10.1007/978-1-4939-0342-9_32,

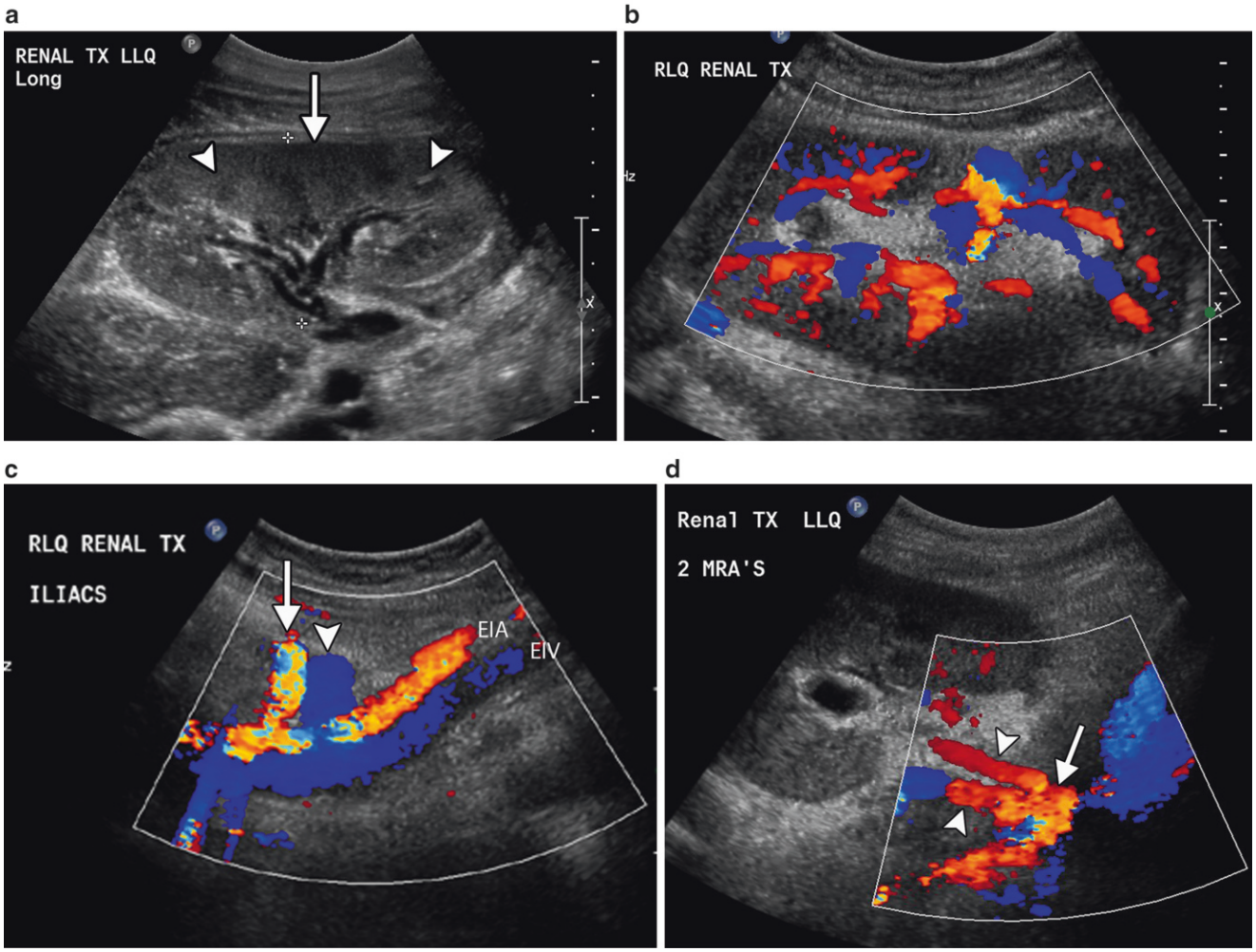

Fig. 32.1 Normal ultrasound. (**a**) Normal gray scale ultrasound obtained in the long axis through the renal transplant. The renal sinus is the bright central echo containing vessels and renal pelvis. It is surrounded by the gray hypoechoic cortex (*arrow*) with darker pyramids (*arrowheads*) at the corticomedullary junction. (**b**) Longitudinal color Doppler image shows flow throughout the allograft. (**c**) Longitudinal color Doppler along the course of the external iliac vasculature shows patency of the arterial (*arrow*) and venous (*arrowhead*) anastomoses to the external iliac artery (*EIA*) and vein (*EIV*). (**d**) Color Doppler image through the renal hilum shows an arterial patch (*arrow*) anastomosed to the iliac artery with two patent renal arteries (*arrowheads*)

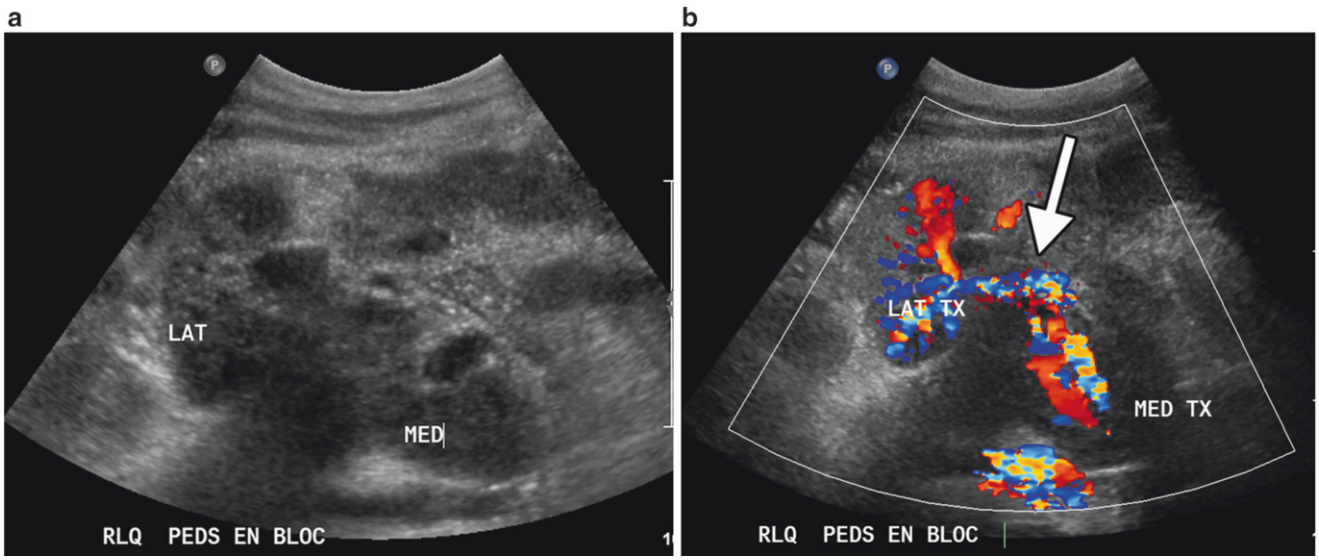

Fig. 32.2 Pediatric en bloc renal transplants. (**a**) Gray scale image of the two renal transplants (*LAT*, *MED*) shows the hila facing each other. (**b**) Color Doppler image shows the vascular anatomy with donor aorta and vena cava (*arrow*)

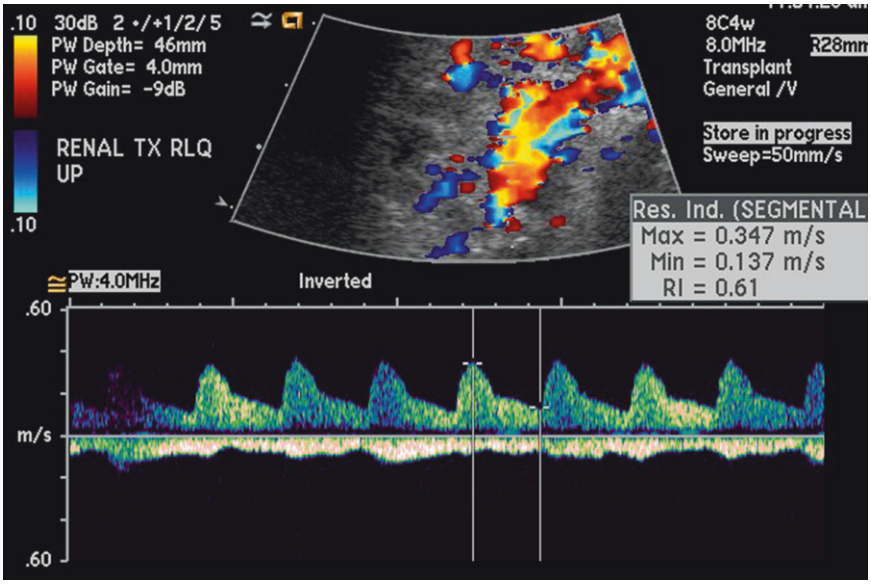

Fig. 32.3 Resistive index. Duplex Doppler tracing of an intrarenal artery demonstrates continuous antegrade, low resistance arterial flow throughout the cardiac cycle. The resistive index has been measured at 0.61

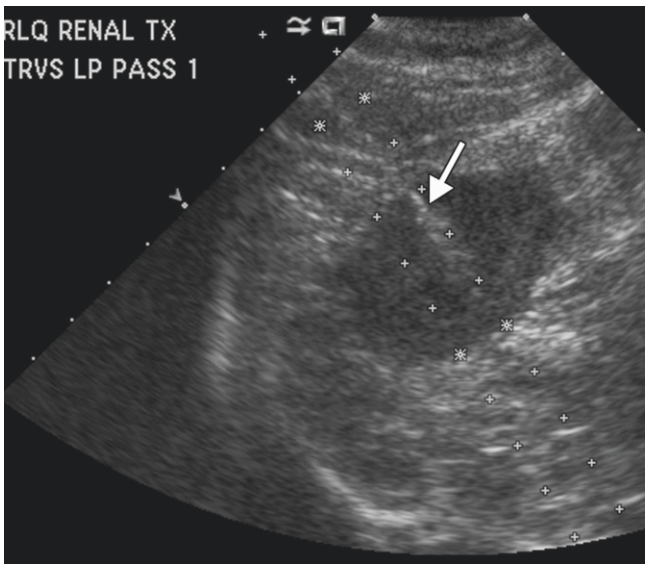

Fig. 32.4 Ultrasound-guided biopsy. The trajectory of the core needle biopsy can be seen in the lower pole peripheral cortex (*arrow*)

Computed Tomography

Computed tomography (CT) utilizes ionizing radiation to produce cross-sectional images with high spatial resolution. In general, computed tomography can be performed in the preoperative assessment of potential recipients and postoperatively for symptoms and signs outside of the renal transplant, e.g., fever, leukocytosis, or gastrointestinal complaints. An optimal CT examination requires iodinated contrast administered orally and intravenously. However, iodinated intravascular contrast may cause contrast-induced nephropathy (CIN) in patients with preexisting renal impairment and diabetes, and its use should be judicious in renal transplant recipients [10, 11]. Elevation in serum creatinine after the use of contrast agents within the early postoperative period is likely multifactorial, with contributory causes including ATN, rejection, cyclosporine toxicity, and dehydration. Prehydration prior to the CT study decreases the risk of contrast nephrotoxicity but does not eliminate it [10]. Although never specifically or adequately evaluated in the renal transplant population, other prophylactic measures such as administration of the antioxidant acetylcysteine are employed by many clinicians in hopes of preventing or reducing the nephrotoxicity of contrast agents.

In the immediate postoperative period, restoration of renal function may be delayed and it is therefore our practice to withhold intravenous contrast until renal function is adequate, or the use of vascular contrast considered absolutely necessary. A stable serum creatinine below 1.5–2.0 mmol/mL [1.5–2.0 mg/dL] or eGFR above 60 mL/min is a general cutoff for administering intravenous contrast media unless clinical urgency dictates the need for contrast-enhanced studies. When indicated, a reduced dose of iodinated contrast may be used. For most postoperative indications such as fever, pain, and diarrhea, an adequate CT study can be obtained without intravenous contrast but preferably with oral contrast. Alternatively, a magnetic resonance study may be substituted, as is discussed later.

CT is excellent for detection and anatomic localization of fluid collections and for guidance of interventional procedures. Transplant biopsies may also be performed using CT guidance instead of ultrasound for deep or less accessible allografts.

A non-contrast CT scan may be useful in evaluating for stones in the native kidney or renal allograft and ureters.

Multidetector CT cystography has become the standard technique for evaluation of traumatic bladder injuries and is now standard at our institution for evaluation of bladder leaks after renal transplantation [12–14]. After a pre-contrast image acquisition, approximately 250–300 mL of diluted iodinated contrast is infused through a Foley catheter and another series of images is obtained when the bladder is distended. CT cystography is highly sensitive to small leaks and 3D multiplanar reformations increase diagnostic confidence. In parallel, CT nephrostography is extremely useful for the diagnosis of ureteral leaks and strictures but requires the prior placement of a percutaneous nephrostomy tube.

Magnetic Resonance Imaging

Magnetic resonance imaging (MRI) is a very versatile modality. MRI can be performed in multiple planes, does not use ionizing radiation, and has high contrast resolution, making it more sensitive than CT to pathologic change within tissues. The use of varying pulse sequences enables tissue characterization (such as fluid, fat, and hematoma) and differentiation of fluid collections. Masses in the allograft and native kidneys or other sites are readily evaluated. MR can detect flowing blood in major vessels without the use of iodinated contrast. In the past, gadolinium-based contrast agents (GBCAs) were considered preferential to iodinated intravascular contrast material in the evaluation of patients with renal failure. GBCAs increased image resolution and improved detection of small vessels allowing the acquisition of high quality angiographic images noninvasively, with a lack of nephrotoxicity [15]. However, current awareness of the association of GBCAs with nephrogenic systemic fibrosis (NSF) in patients with reduced renal function has significantly impacted the use of GBCAs, requiring careful screening of patients at risk and tailoring of examinations to maximize useful information while minimizing exposure.

Non-contrast-dependent angiographic techniques based on fast spin-echo, gradient-echo, phase-contrast, and inversion-recovery principles have been developed or maximized to assess the renal transplant vasculature, including ECG-gated 3D non-enhanced magnetic resonance angiography (MRA) performed with selective inversion-prepared fast imaging with steady state free-precession (TrueFISP). This has been shown to depict the renal transplant arteries comparable to contrast-enhanced MRA [16, 17], and is used most commonly at our institution. When contrast-enhanced MRI is unavoidable, the dose and type of GBCA should be carefully selected to minimize risk, as recent studies have shown that when restrictive GBCA administration guidelines based on glomerular filtration rate (GFR) are followed, the incidence of developing NSF significantly decreases [18].

Functional MRI of renal allografts is a field of active research. MR techniques such as contrast-enhanced perfusion imaging, diffusion-weighted imaging, BOLD (blood oxygen level-dependent) imaging, and arterial spin labeling are available to measure perfusion, blood oxygen level, and GFR [19–22]. This has great potential in the noninvasive diagnosis of transplant dysfunction. Newer techniques such as MR elastography which measures tissue stiffness may in future play a role in the detection and quantification of fibrosis [23]. Diffusion-weighted imaging has become increasingly useful in the detection and staging of cancer with future potential in tissue characterization and grading of neoplasms and lymphadenopathy [24].

MRI is contraindicated in patients with most pacemakers and some metallic implants such as intracranial aneurysm clips and heart valves. Patients with claustrophobia may be unable to tolerate MRI despite sedation. Other disadvantages of MRI include the cost, availability, and relative length of the studies. Many of the newer sequences are breath held and require patient cooperation. Artifacts from surgical clips and stents may degrade image quality and cause spurious stenoses [25, 26].

Nuclear Scintigraphy

Nuclear scintigraphic renal studies are of value for the assessment of renal allograft function. For many years, technetium 99m pentetate (DTPA) was the most frequently used radiopharmaceutical for evaluation of renal allografts. In the last decade, this agent has been replaced by technetium 99m mertiatide (MAG3). Technetium 99m MAG3 is an agent that undergoes predominantly tubular secretion, and is a more efficient imaging agent than technetium DTPA. Images are obtained over the kidney immediately after the intravenous injection of technetium MAG3 to assess perfusion of the transplant, with development of perfusion parameters for quantitative evaluation [27]. Normal, decreased, or absent allograft renal blood flow may be calculated by comparison of the intensity of radiotracer activity over the kidney with the adjacent aorta or iliac blood vessels. GFR and effective renal plasma flow (ERPF) may be calculated. However, serial studies are often necessary in the determination of abnormal renal perfusion and ideally, a baseline MAG3 study is obtained within several days of the transplantation. Study quality may be compromised by poor hydration, and evaluation of the transplant may also be limited by uptake and secretion of MAG3 within the native kidneys if these remain partially functional.

Renal transplant vascular complications may be identified during the perfusion phase of technetium MAG3 studies although these abnormalities are more optimally evaluated and detected with Doppler ultrasound techniques.

Delayed scintigraphic imaging of the renal transplant is obtained after 30 min. The secretion of MAG3 into the renal

collecting system, ureter, and bladder is measured and imaged. MAG3 studies remain very helpful for the detection of urinary leak and ureteral obstruction that most often occur at the anastomosis of the transplant ureter to the recipient bladder. MAG3 studies may also be helpful in the detection of vesico-ureteric reflux. This complication is frequently seen in transplanted kidneys due to the absence of a sphincter at the ureterovesical junction. Radiotracer intensity over the ureter and kidney may alternate over time due to periodic reflux of radiotracer-labeled urine from the bladder into the ureter and renal pelvis.

Isotope renography can be used to investigate renal dysfunction. In ATN, perfusion is normal but excretion is delayed and decreased. With rejection both perfusion and excretion are abnormal. However since other causes of graft dysfunction may have a similar picture, isotope renography is not of major value for the detection of rejection in transplant kidneys.

Interventional Radiology

While conventional catheter-based angiography remains the gold standard for the diagnosis of arteriovenous fistulae, pseudoaneurysms, and renal artery or vein stenosis, in practice, vascular abnormalities are usually initially detected by Doppler ultrasound and may be confirmed by MR or CT angiography. Instead, conventional angiography with digital subtraction techniques is reserved for confirmation of suspected abnormalities immediately prior to percutaneous transcatheter interventions such as angioplasty and stent placement in transplant artery stenosis or embolization of a fistula [28, 29]. Allograft arterial and venous thrombosis is usually diagnosed by ultrasound and the role of interventional radiology is limited to mechanical thrombectomy and catheter-directed thrombolysis in select cases [30, 31].

The limitations of conventional angiography include the relative invasiveness and the required use of nephrotoxic iodinated intravascular contrast media. To limit the nephrotoxicity of administered iodinated contrast, catheter-based angiography can be performed using low doses of low- or iso-osmolar contrast material [32], possibly in conjunction with carbon dioxide gas, which has been used as a sole intravascular agent but has poor image contrast [33, 34]. Although GBCAs have historically been used as intra-arterial angiographic contrast agents, given the emergence of NSF and the relatively high doses needed for equivalent radio-opacity, they are no longer acceptable in patients with renal dysfunction [32].

Interventional radiologists play an invaluable role in the postoperative management of transplant-related complications by performing endovascular treatment, percutaneous urinary intervention, and abscess or fluid drainage [32, 35–37], as will be addressed later under the specific complication.

Radiography

There is a limited role for abdominal radiography, limited to evaluation of stents, foreign bodies, renal calculi, and bowel complications. Chest radiography is widely used postoperatively.

Pre-transplant Work-up

Patients with long-standing renal disease often have many comorbidities which can affect graft and patient survival. Given the high demand for, and shortage of, donated kidneys, pre-transplant screening plays an important role in detecting coexisting illnesses and to evaluate feasibility of transplantation. This evaluation typically includes complete history and physical examination, with appropriate laboratory testing and up-to-date preventative health measures including colonoscopy and/or mammograms [38]. Basic radiologic imaging, including chest radiograph and abdominal ultrasound, is usually performed with more advanced imaging dictated by historical or clinical factors.

In many centers, preoperative contrast-enhanced CT arteriography (CTA) of the abdomen and pelvis is obtained in potential recipients. Selection criteria include age >50, chronic renal disease caused by diabetes and hypertension, known history of atherosclerosis or identification of atherosclerotic calcifications on radiography, or prior transplantation [39]. Important considerations include potential need for pre-transplant nephrectomy; evaluation for preexisting renal cell carcinoma or other malignancy, particularly in the dialysis population; and evaluation for sufficient atherosclerotic plaque-free patent vasculature for vascular anastomoses. In patients already on dialysis, normal dose contrast-enhanced CTA is performed. For patients who are predialysis, the risk of CIN can be lessened by hydration, before and after contrast administration [11, 40–42]. A recent study using 50–60 % of the standard dose of contrast for CTA with pre- and post-procedural hydration did not result in development of CIN in patients not yet on dialysis [43]. Additionally, at our institution, we are evaluating the potential of low kV (80 kV) CT scanning to potentiate lower doses of intravenous contrast (less than half the standard dose of 100 cc). Oral contrast is not administered as the high density interferes with volume rendering and creation of 3D reconstructions used for evaluation and presurgical mapping of vascular calcification.

Additionally, using CT, the native urinary tract can be assessed to determine need for concurrent nephrectomy (i.e., polycystic kidneys) or the presence of malignancy, given increased risk of renal cell carcinoma in the long-term dialysis-dependent patient [44].

Post-transplant Imaging Evaluation

The use of routine postoperative imaging is institution dependent. Common indications for imaging are absent or decreased urine output, delayed graft function, rising or persistently elevated creatinine, fever, pain over the allograft, or drop in hematocrit. Hypertension or hematuria may also prompt imaging evaluation. Patients with delayed graft function may have baseline imaging studies prior to discharge, which can be useful for comparison when follow-up studies are obtained. Ultrasound is the most commonly performed modality due to its unique advantages previously described. However CT, scintigraphy, and MR are complementary modalities in the radiologic armamentarium.

Complications After Renal Transplantation

Immediate complications, occurring in the first week, are mostly related to the surgical procedure and include renal artery or vein thrombosis, hemorrhage, and ureteral edema. Nonsurgical complications consist mainly of ATN and acute rejection. Early complications occur between 1 week and 1 month and include acute rejection, urinary leak, infection, fluid collections, and vascular thrombosis. After 1 month, lymphoceles, acute or chronic rejection, ureteral strictures, renal artery stenosis, infection, cyclosporine toxicity, recurrence of renal pathology, and neoplasms form the bulk of problems likely to be encountered. Overall, the most common complications are perinephric fluid collections which occur in up to 50 % of recipients [45, 46]. General complications relating to abdominal surgery are also encountered and include postoperative ileus, bowel obstruction, venous thromboembolic disease, and infections (systemic, pulmonary, renal, or bowel in origin). CT is the most useful imaging study when searching for infection or in patients with nonspecific chest or abdominal symptoms. Ultrasound is the study of choice for extremity deep venous thrombosis but is limited in the upper mediastinum or pelvis. For suspected thoracic, pelvic, or inferior vena cava thrombus, CT with contrast or MRI is the preferred modality. Multidetector CT pulmonary arteriography is the study of choice for pulmonary embolism.

Parenchymal Complications

Parenchymal complications include rejection, acute or chronic, delayed graft function, and calcineurin inhibitor toxicity. Time of onset of graft dysfunction and measurement of calcineurin inhibitor levels may be diagnostically helpful in distinguishing these complications. However in the majority of cases with elevation of serum creatinine or decreased urine output, ultrasound with Doppler is essential to exclude vascular and urologic complications.

Rejection

Since the development of more effective perioperative multidrug immunosuppressive therapies as well as the essential elimination of hyperacute rejection with modern cross matching techniques, rejection occurs less often in the first week after surgery. However, rejection remains a frequent cause of allograft dysfunction after that time and has a cardinal impact on patient and graft survival.

Despite early claims that altered transplant echogenicity, increased corticomedullary differentiation, and other subtle gray scale changes were predictive of acute rejection, it is now generally agreed that there are no specific gray scale sonographic characteristics of acute rejection [47, 48]. Allograft swelling and elevated resistive index (RI values > 0.8) or absent diastolic flow on Doppler arterial evaluation may be observed at sonography (Fig. 32.5a, b), but these findings are neither sensitive nor specific in the acute setting [49–52]. In one study, more than 50 % of allografts with biopsy-proven rejection had normal RIs of 0.7 or less [52]. The problem is that the RI is calculated in larger arteries, such as the interlobar or arcuate artery, and is interpreted as indirect evidence of disease at the capillary level. Unfortunately, there is susceptibility to error resulting from the effect of systemic disease, such as atherosclerosis, and renal artery stenosis [53]. Since acute rejection of a kidney graft primarily involves the subcapsular capillaries, early and detailed evaluation of blood flow in this area is highly desirable [54].

Continued technical developments in US imaging and the introduction of ultrasound-specific contrast medium (microbubbles) have shown promise for the assessment and quantification of microvascular perfusion. Several studies have shown direct correlation of delayed parenchymal perfusion with pathologically proven rejection, compared to perfusion dynamics seen in patients with normal function or ATN [53–55]. However, more research needs to be done, and until ultrasound contrast medium is approved for use in the US, this work remains "in progress" [8, 9]. Therefore, at this time, the main value of ultrasound in acute transplant dysfunction is to identify ureteric obstruction or vascular complications such as ischemia or thrombosis as the underlying cause. If these potential causes of allograft dysfunction have been excluded, percutaneous biopsy with sonographic guidance is usually performed to determine the specific etiology (Fig. 32.4). Nuclear scintigraphy, CT, and MRI are not of value in this setting.

Chronic Rejection

Chronic rejection is one of the most common causes of renal allograft failure [56]. It may present after a few months, and usually is detected because of elevated serum creatinine, often with proteinuria. Ultrasound is performed to exclude

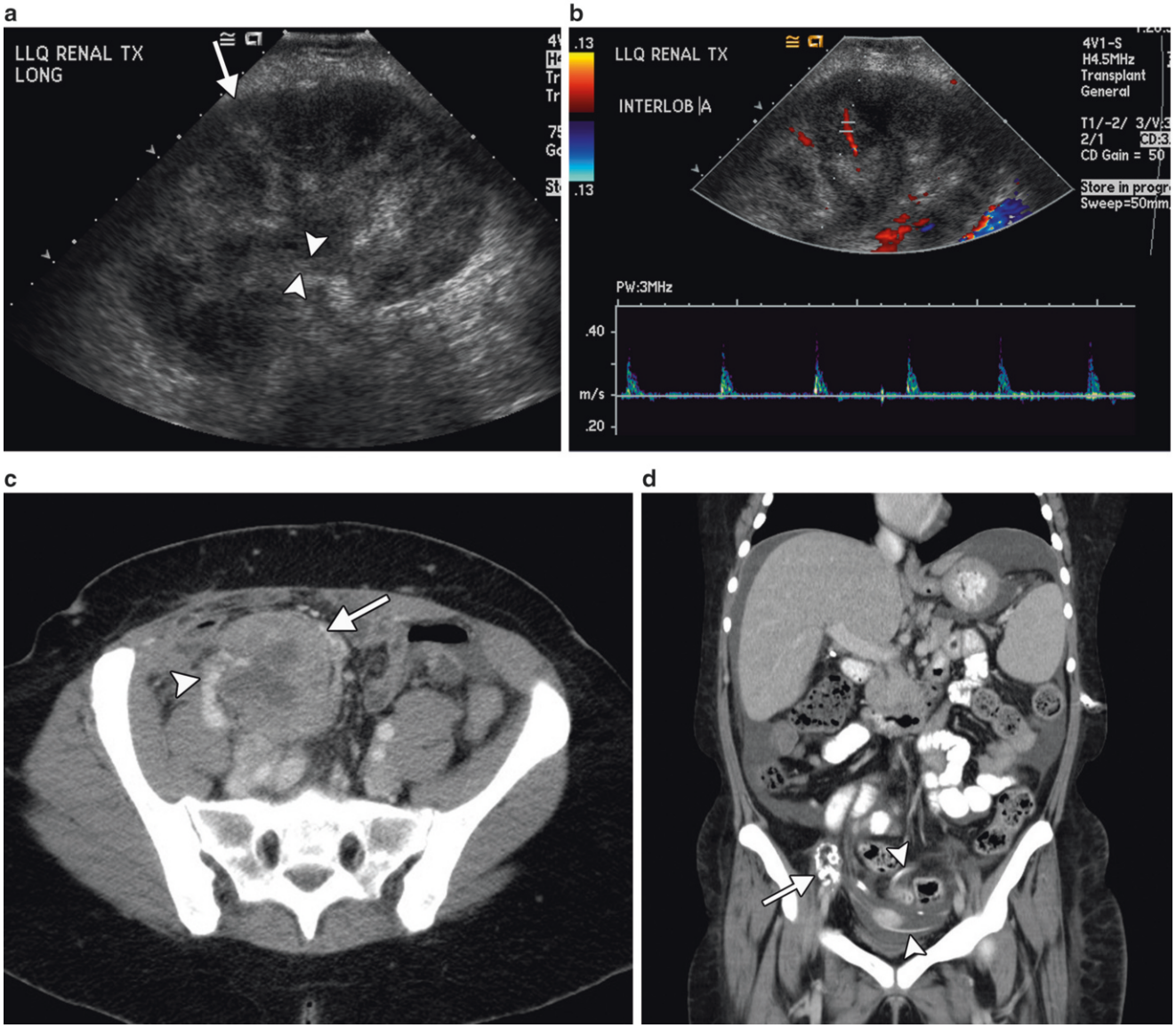

Fig. 32.5 Failed renal transplants. (**a**) Longitudinal gray scale ultrasound shows an enlarged, globular renal transplant with increased parenchymal echogenicity (*arrow*) and urothelial thickening (*arrowheads*). (**b**) Color and spectral Doppler imaging shows poor color flow and high resistance arterial waveforms with no diastolic flow. (**c**) Axial contrast enhanced CT through the pelvis shows an enlarged renal transplant (*arrow*) with patchy enhancement and patent vasculature (*arrowhead*), nonspecific imaging findings in a patient with biopsy proven acute on chronic rejection. (**d**) Coronal maximum projection-reconstructed CT image shows an atrophic calcified renal transplant (*arrow*) in the right lower quadrant. Also noted is a peritoneal dialysis catheter in the pelvis (*arrowheads*) and associated abdominopelvic ascites

structural causes of dysfunction. The allograft may be normal in size on ultrasound, but over time is likely to become progressively atrophic. A thin hyperechoic cortex with sparing of the medullary pyramids may be seen in advanced cases. As with acute rejection, Doppler arterial waveforms may be normal. However in a recent study, Doppler arterial resistive index measurements above 0.8 in a segmental branch on a single occasion more than 3 months after transplantation have been shown to be predictive of eventual graft failure [7]. Chronic rejection may be difficult to differentiate from acute rejection and cyclosporine toxicity on the basis of ultrasound findings, and unless the allograft is atrophic and calcified (Fig. 32.5d), with decreased color flow, percutaneous biopsy using sonographic guidance is usually performed to determine the cause.

Delayed Graft Function/Acute Tubular Necrosis

ATN is the most common cause of delayed graft function in the first week after surgery. Imaging is generally performed to exclude other causes of poor graft function as there are no specific imaging characteristics of ATN. Allograft swelling and elevated resistive index may be observed at sonography, but are nonspecific. As mentioned previously in the rejection section, contrast-enhanced ultrasound allows for assessment

of the allograft microperfusion, and several studies have shown abnormal perfusion dynamics in patients with biopsy-proven ATN, compared to normal early graft function and acute rejection [9, 53]. Although the early results are interesting, more research is required, and biopsy remains the diagnostic gold standard [8]. At nuclear scintigraphy, relative preservation of perfusion with impaired clearance of tracer is noted [57, 58].

Vascular Complications

Up to 3 % of renal transplant recipients develop vascular complications [59, 60] with 66 % occurring within 1 month of transplantation. Early complications include renal artery or vein thrombosis, renal artery kinking or compression by collections, and hemorrhage. Renal artery thrombosis is the most common vascular cause of graft loss. After 1 month, the most common complication is renal artery stenosis. While not uncommon, biopsy-related complications such as arteriovenous fistulae are likely to resolve spontaneously and are not as clinically significant. Less common complications are renal vein stenosis and renal torsion [61].

Renal Vascular Thrombosis

Renal vein and renal artery thrombosis present with acute deterioration in graft function and urine output. Doppler ultrasound is the study of choice. An infarcted allograft will be swollen without evidence of parenchymal flow at color or spectral Doppler (Fig. 32.6a). With complete arterial thrombosis, there will be no detectable arterial flow in the allograft but a spiked preocclusive waveform may be detected in the renal artery proximal to the clot [2, 45, 62]. When there is more than one renal artery, accessory renal artery thrombosis may be suspected by failure to detect flow in all the arteries and by segmental absence or decrease of color flow in the renal parenchyma (Fig. 32.6b). Segmental infarcts may be wedge shaped and hypoechoic.

In early stage venous thrombosis, the renal artery may still be patent with Doppler showing an abnormally high resistance waveform and reversal of flow in diastole (Fig. 32.7) [63, 64]. Confirmation of renal artery or vein thrombosis with other imaging modalities is rarely required and delays surgical management. There is rarely a role for interventional radiologic thrombolysis.

Dissection of the main renal artery is rare. It is usually associated with technical intraoperative difficulties. The dissection flap will not usually be detected by ultrasound; however, decreased color flow and decreased peak velocities are indirect signs (Fig. 32.8a). CTA, MRA, or conventional angiography is superior for diagnosis (Fig. 32.8b) [65]. Treatment may be attempted by angioplasty and percutaneous stent placement (Fig. 32.8c) [65].

Severe acute rejection can increase intrarenal resistance resulting in elevated high peak systolic velocity and reversal or loss of diastolic flow [2, 45, 66]. This may culminate in thrombosis.

Renal Artery Stenosis

It is not uncommon to have mild to moderate vessel narrowing at the arterial anastomosis in early postoperative period [67]. Close follow-up is recommended rather than intervention. Later, renal artery stenosis is the most common vascular complication of renal transplantation, occurring in 0.51–12 % of recipients and usually within 1 year [29, 59, 60, 68, 69]. Typical presenting features are hypertension and graft dysfunction, and occasionally a bruit. A hemodynamically significant stenosis is one which narrows the lumen by 50 %. The site of the stenosis can be at the anastomosis (in 50 %), in the donor artery, or on the recipient side. Etiology is multifactorial with contributory factors including atherosclerosis, surgical trauma and technique (e.g., torsion or angulation at the vascular anastomosis), rejection, and infection.

Ultrasound is very useful as a noninvasive screening tool. The iliac artery, renal artery anastomosis, and entire renal artery are evaluated with color Doppler for areas of altered color flow and aliasing (disturbance of color signal because of elevated velocity). Peak systolic velocity is measured at multiple sites to determine the highest peak systolic velocity. The most commonly used Doppler criteria for renal artery stenosis include an elevation of peak systolic velocity to 2–2.5 m/s (Fig. 32.9a), a velocity gradient between the stenotic and non-stenotic segments greater than 2:1, or a ratio of peak systolic velocity in the renal artery to external iliac artery (EIA) of 1.8–2 [70, 71]. In a high-risk population, these criteria achieve a sensitivity of 87–94 % and specificity of 86–100 % [45, 70, 72, 73]. However in a low risk population, the false-positive rate is high when a threshold of 2.5 m/s is used and follow-up rather than angiography should be considered [74]. Kinking and tortuosity may cause a spurious elevation of peak systolic velocity (Fig. 32.10).

Due to technical difficulty in evaluating the renal artery anastomosis in some patients, indirect evaluation of renal artery stenosis can also be performed. Intrarenal arterial waveforms are evaluated for a delayed acceleration time (pulsus tardus) and slow rise to peak (pulsus parvus) (Fig. 32.9b). Threshold values in common use include a resistive index below 0.55 [45, 71], an acceleration time greater than 0.07–0.1 s [75]. Of note, these criteria are not applicable to pediatric transplants [76].

Catheter contrast angiography (with digital subtraction) is the reference standard for diagnosis and grading of renal artery stenosis (Fig. 32.9c). Pressure measurements can be performed to determine the significance of areas of narrowing and treatment can be performed at the same time. However angiography is invasive and requires contrast medium.

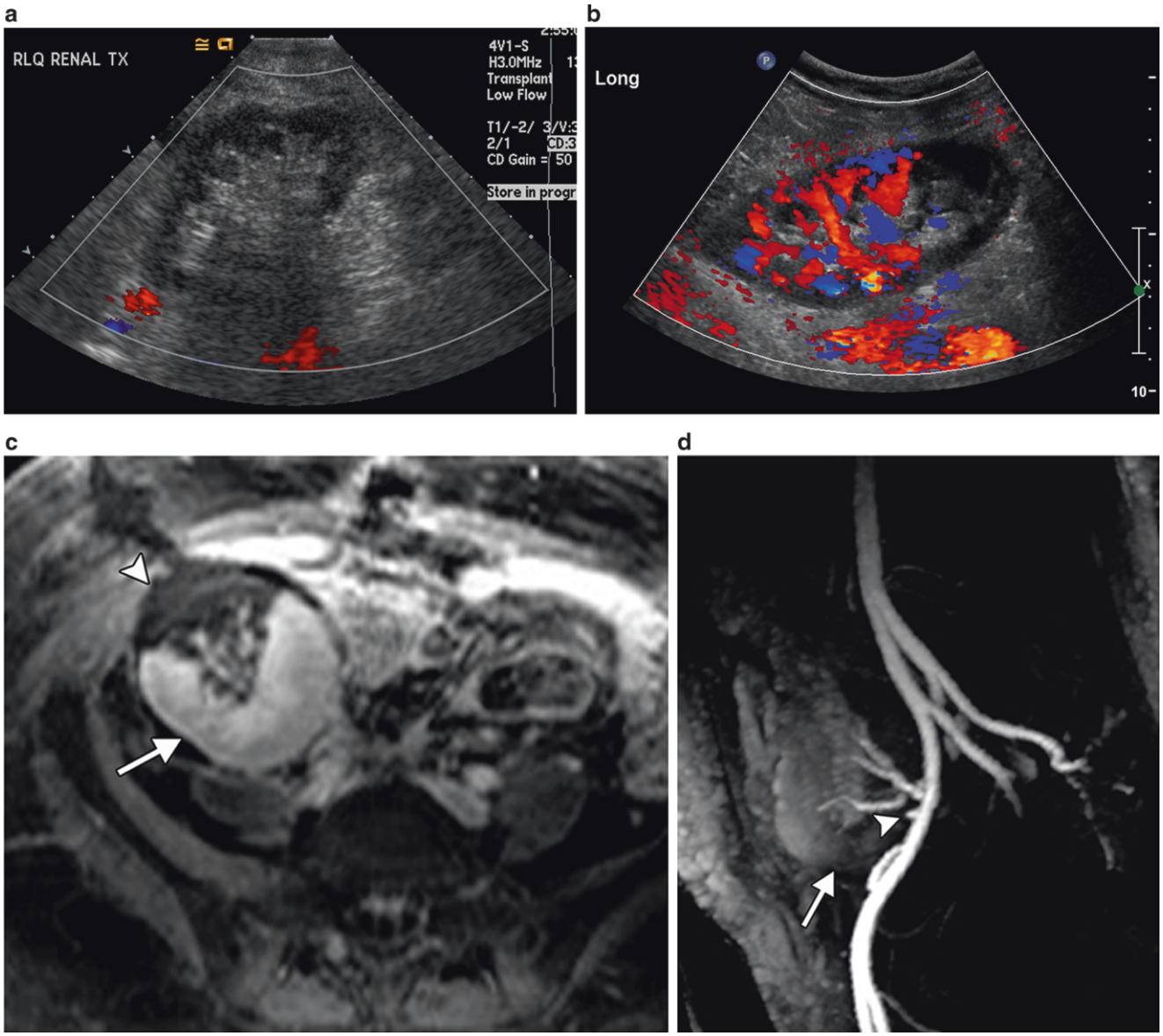

Fig. 32.6 Renal artery thrombosis. (**a**) Longitudinal color Doppler image shows the absence of color flow throughout the renal transplant. (**b**) Longitudinal color Doppler image shows segmental lower pole ischemia secondary to thrombosis of one renal artery in a patient with two renal arteries. (**c**) Fat suppressed, post-contrast T1 weighted MR image shows a wedge-shaped area of non-perfusion (*arrowhead*), with normal enhancement of the remainder of the transplant (*arrow*). (**d**) MRA shows occlusion of the inferior renal artery (*arrowhead*), with no enhancement of the lower pole (*arrow*)

Furthermore multiple injections and projections are necessary to analyze the aortoiliac segments and for tortuous or overlapping vasculature.

CT or MR contrast angiography may be performed prior to catheter angiography, in cases of non-diagnostic ultrasound or as a screening test. These modalities have the advantage of a wider field of imaging to include the entire aortoiliac and pelvic vasculature (after a single bolus of intravenous contrast) with the ability to manipulate the data in three dimensions. They are accurate in the diagnosis of transplant renal artery stenosis. Contrast-enhanced MRA is reported to have a sensitivity of 93.7 %, specificity of 80 %, accuracy of 88.5 %, positive predictive value of 88.2 %, and a negative predictive value of 88.9 % when compared to angiography (Fig. 32.11a) [15]. Pseudorenal artery stenosis from iliac stenosis and diffuse atherosclerotic disease may be detected, as well as perfusion defects and infarcts [26]. MRA may be limited by artifacts caused by certain arterial stents and metallic surgical clips. These cause signal loss and may prevent evaluation of vascular patency (Fig. 32.11b) [26]. Additionally MIP reconstruction techniques may overestimate degree of stenosis [26]. In allograft recipients with poor renal function, non-contrast MRA may be extremely helpful (Fig. 32.11c) [77–79].

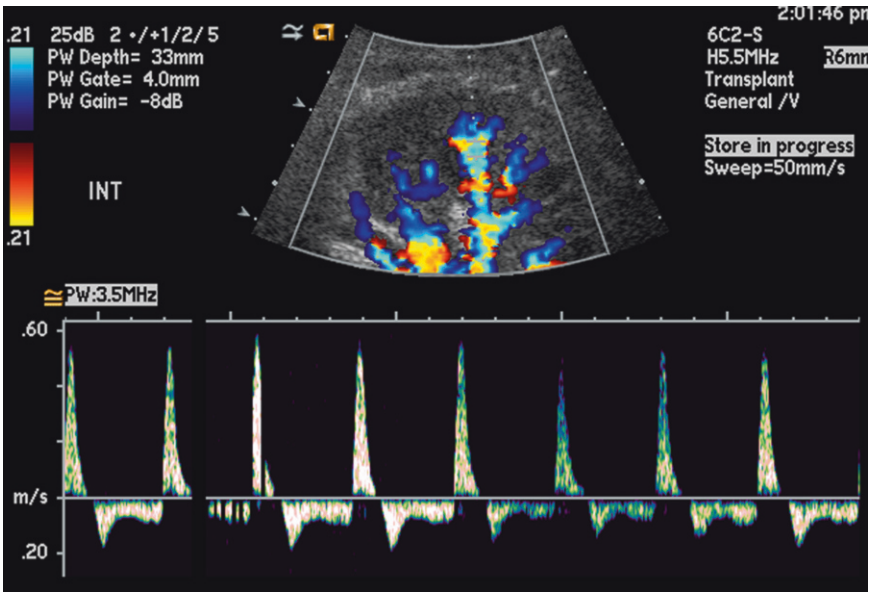

Fig. 32.7 Renal vein thrombosis. Duplex Doppler waveform shows high systolic arterial peaks with reversal of flow in diastole

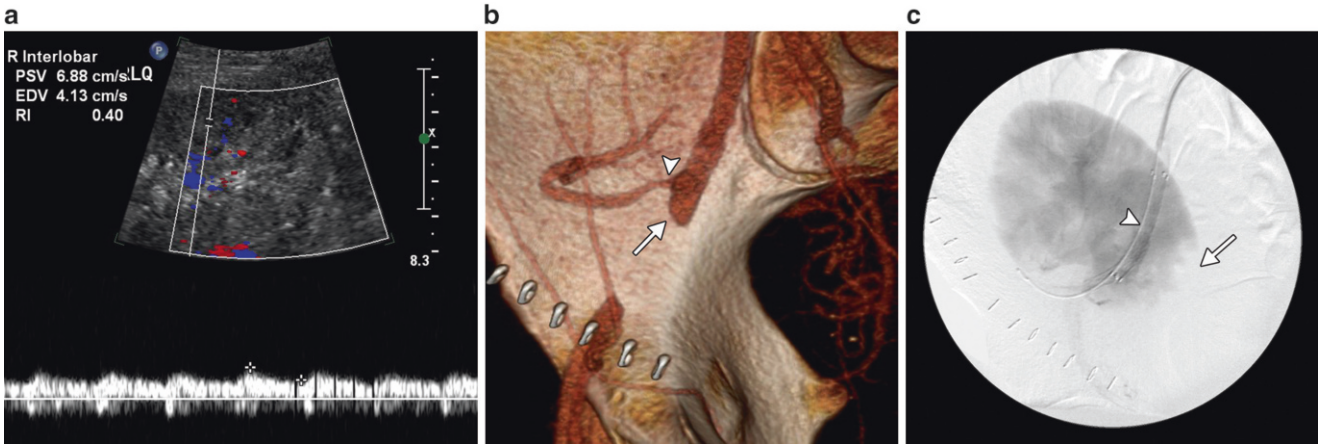

Fig. 32.8 Renal and iliac artery dissection. Doppler ultrasound shows a dampened intrarenal arterial waveform with a low resistive index of 0.40 (**a**). CT arteriogram shows occlusion of the EIA (*arrow*). There is stenosis of the transplant renal artery (*arrowhead*) (**b**). Digital subtraction image confirmed the findings which were treated with stents. Note the stent (*arrowhead*) and the lower pole infarct (*arrows*) (**c**)

Renal artery stenosis is initially treated by percutaneous transluminal angioplasty (PTA) with a success rate of 85–93 % and a complication rate of 4 % [32]. Complications include dissection, arterial rupture, and thrombosis. Restenosis occurs in 5–30 %, and may be treated by repeat PTA with or without stenting. Stenoses which are not amenable to or have failed endovascular approaches are managed surgically. Arterial kinks do not respond to endovascular techniques and typically require surgery [60]. Stenosis in the iliac artery above the main renal artery may impair graft function, and can also be treated with PTLA or stent.

The findings at radionuclide scintigraphy are not specific, and captopril renography is of limited diagnostic value in this setting.

Compartment Syndrome

An uncommon cause of early graft dysfunction is the renal compartment syndrome [80, 81]. Compression of the allograft in the pelvic cavity results in abnormal perfusion with reversed or absent diastolic flow and venous outflow obstruction (Fig. 32.12). Early diagnosis permits graft salvage.

Arteriovenous Fistulae and Pseudoaneurysm

Intrarenal arteriovenous fistulae are not uncommon after percutaneous biopsy, reportedly occurring in 1–18 % of biopsies [32, 60]. Pseudoaneurysms are less common. Both may be clinically silent and discovered incidentally by Doppler ultrasound. Typical presentation is gross hematuria after a biopsy.

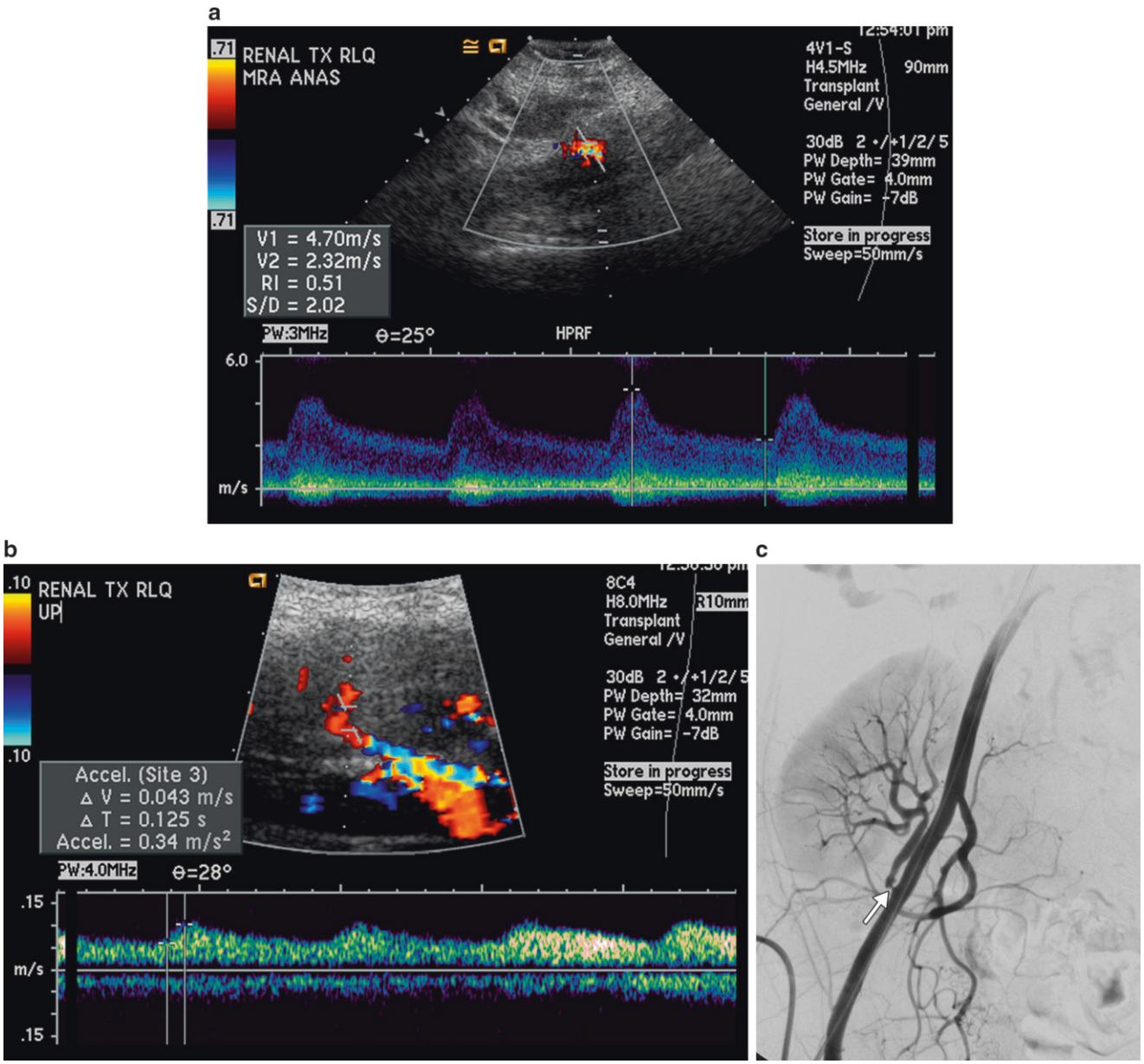

Fig. 32.9 Renal artery stenosis. (**a**) Duplex waveform at the renal artery anastomosis shows elevation of peak velocity, measuring 4.7 m/s. (**b**) Intrarenal waveform has a tardus–parvus pattern with decreased acceleration index and increased acceleration time of 0.125 s. (**c**) Catheter angiography confirming stenosis (*arrow*)

Rarely, hemorrhage, shunting, and graft dysfunction may occur. Extrarenal arteriovenous fistulae and pseudoaneurysms are secondary to surgical technique and are very rare.

On gray scale sonography, arteriovenous fistulae are usually invisible unless large when they appear as anechoic tubular or round structures. Color Doppler characteristics include a focal area of color aliasing with high velocities and perivascular turbulence manifest as a color "flurry" which may be transmitted to the surrounding tissues (Fig. 32.13a). Doppler waveforms show a characteristic high velocity, low resistance arterial waveform in the feeding artery and an arterialized venous waveform (Fig. 32.13b) [2, 45, 82]. The feeding artery and vein are generally not resolved with Doppler sonography, unless large. As many arteriovenous fistulae resolve spontaneously, management is initially conservative. Large or symptomatic arteriovenous fistulae can be treated by transcatheter embolization with metallic coils. Selective arteriography is initially performed to determine the road map (Fig. 32.13c). Success rates are high with minimal loss of parenchyma and few procedural complications [32, 83].

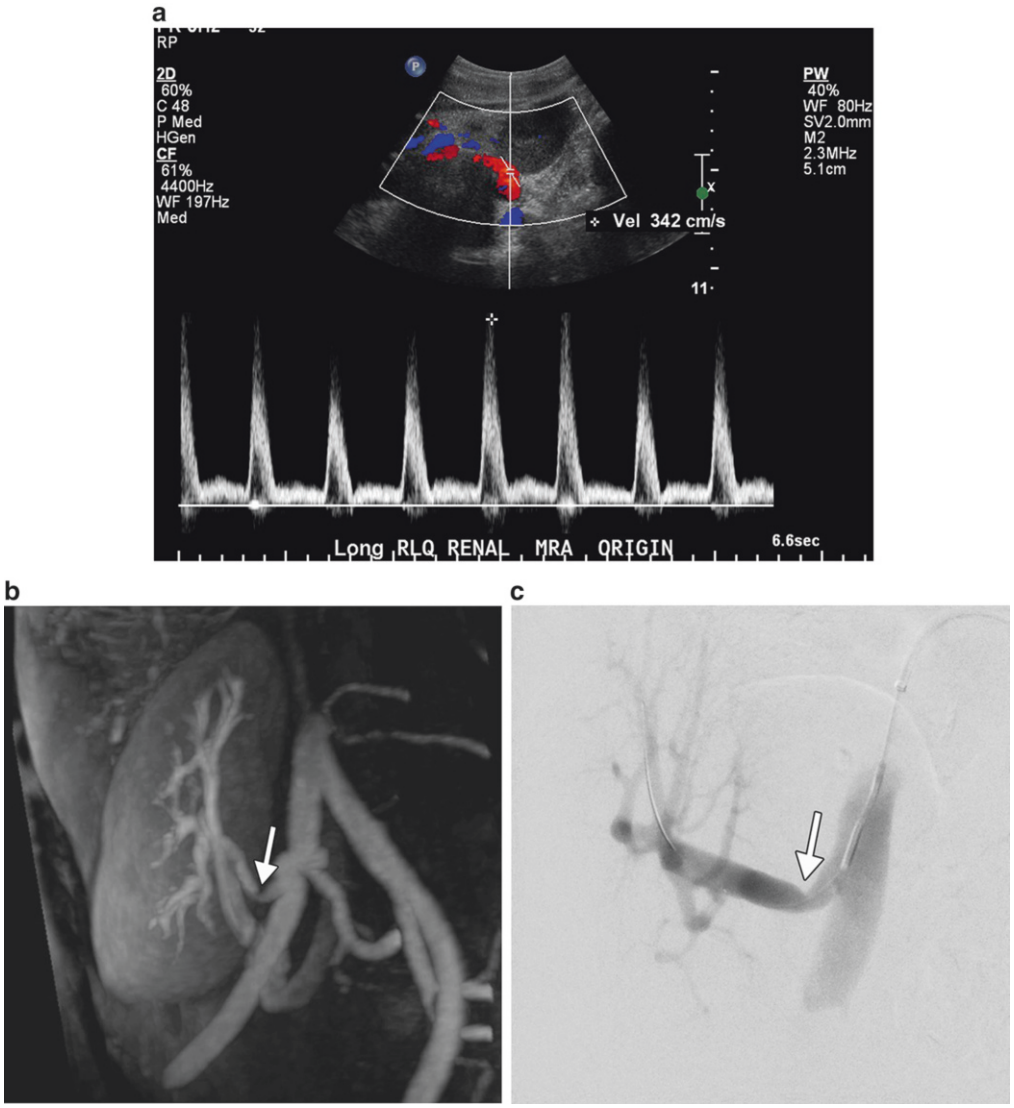

Fig. 32.10 Renal artery kink. (**a**) Duplex waveform shows elevation in peak velocity in the proximal renal artery, measuring 342 cm/s. (**b**) MRA performed without contrast shows angulation of the proximal renal artery (*arrow*) which was proven to be a kink (*arrow*) at angiography (**c**)

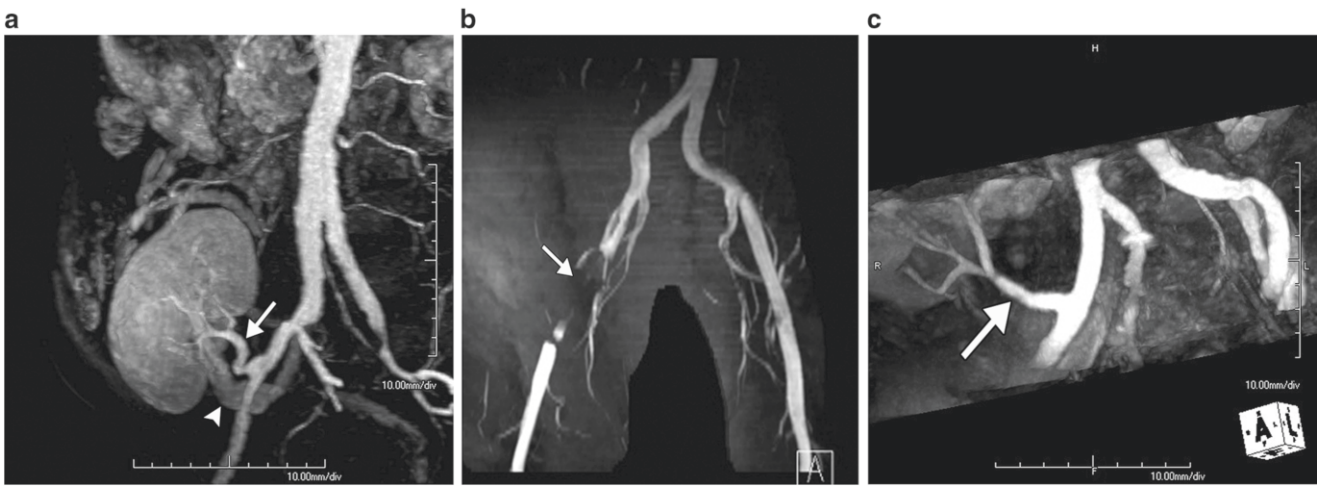

Fig. 32.11 MRA. (**a**) Oblique reconstruction of contrast-enhanced MRA of the pelvic arterial supply demonstrates a normal renal artery (*arrow*) with minimal aortoiliac atherosclerosis. Incidentally noted is opacification of the main renal vein (*arrowhead*). (**b**) Contrast-enhanced MRA performed after stenting of iliac artery dissection. Loss of signal is noted at the level of the stent (*arrow*), precluding evaluation of the lumen. (**c**) Oblique reconstruction of non-contrast MRA of the pelvic arterial supply demonstrates a normal renal artery (*arrow*)

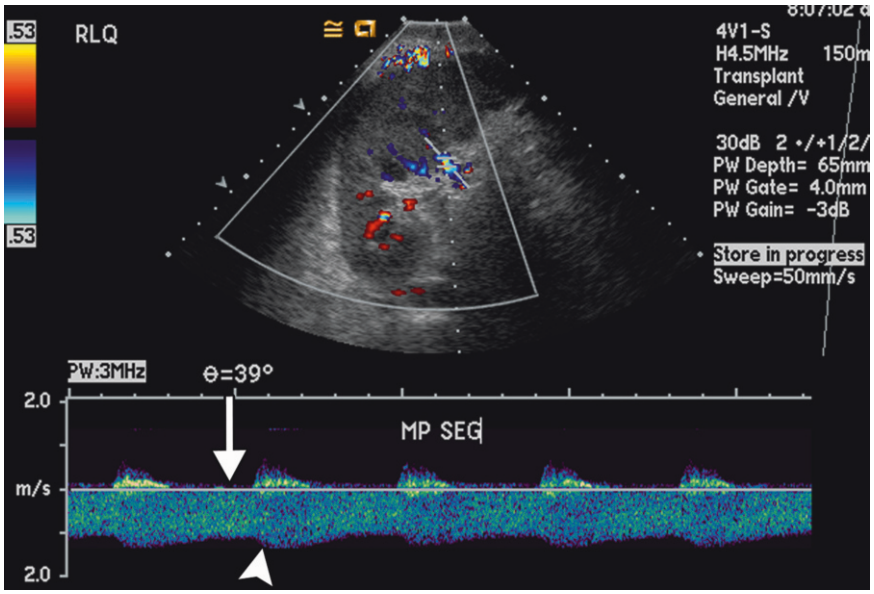

Fig. 32.12 Compartment syndrome. There is global decrease in color flow throughout the renal transplant. The arterial waveforms (*arrow*) show loss of diastolic flow but there is elevation of the velocity in the segmental vein (*arrowhead*)

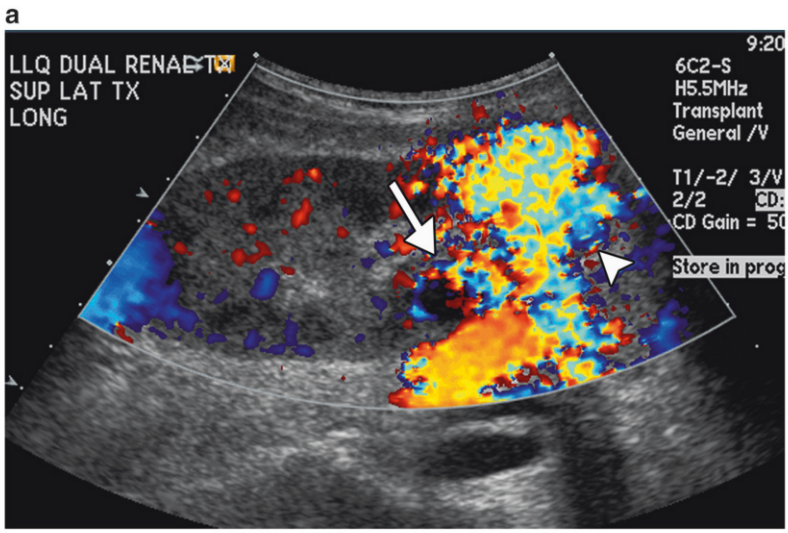

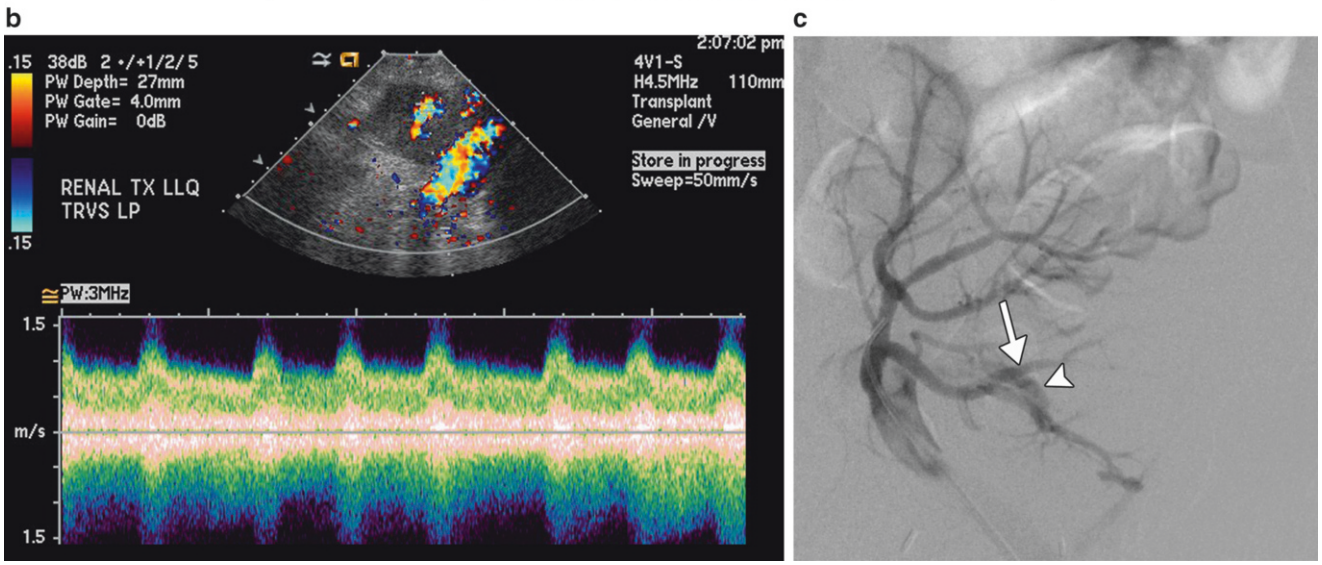

Fig. 32.13 Arteriovenous fistula. (**a**) Longitudinal color Doppler image shows a large lower pole arteriovenous fistula (*arrow*) with perivascular color flurry (*arrowhead*). (**b**) Duplex Doppler shows high velocity, low resistance arterial flow. (**c**) Digital subtraction selective renal artery angiogram showing an abnormal communication between an interlobular artery (*white arrow*) and early filling of an adjacent renal vein (*arrowhead*)

Pseudoaneurysms may appear as a simple or complex cyst on gray scale ultrasound (Fig. 32.14a). Specific Doppler characteristics are "yin yang" swirling flow within the pseudoaneurysm sac and to and fro flow on Doppler interrogation of the neck of the pseudoaneurysm (Fig. 32.14b, c) [2, 45]. Pseudoaneurysms may coexist with arteriovenous fistulae. Extrarenal pseudoaneurysms tend to occur at the arterial anastomosis either from surgical technique or from surrounding infection. They are more prone to rupture. Pseudoaneurysms of both types may be treated by embolization although large extrarenal pseudoaneurysms are difficult to treat and may require surgery (Fig. 32.14d, e).

Renal Vein Stenosis

This is a rare complication, usually resulting from perivascular fibrosis or compression by fluid collections. Fibrosis is difficult to treat by venous angioplasty as recoil is a problem. Primary stenting may be better [29, 84]. Gray scale findings include luminal narrowing or venous compression by a fluid collection. Doppler findings are more specific, and consist of aliasing on color Doppler and a focal velocity increase at the venous stenosis. To be significant, the velocity at the stenosis must be three to four times higher than in the normal venous segment [66]. Collateral veins may suggest the diagnosis. Arterial perfusion and diastolic flow may also be reduced.

Urologic Complications

Urologic complications occur in up to 6 % of recipients. The most common are ureteral stricture and leak which may be secondary to surgical technique, ischemia, and necrosis [59, 85, 86]. Other complications include ureteral or bladder stones and bladder outlet obstruction [85].

Hydronephrosis develops in 3–6.5 % of patients [87, 88] and may be early or late. In the early postoperative period, hydronephrosis may be secondary to edema, clot, calculus, or extrinsic compression by collections, hematoma, or an overdistended bladder. Later, ureteral strictures from ischemia, fibrosis, rejection, or infection (including BK virus (BKV) infection) predominate [28, 88]. Ureteral obstruction is caused by an ischemic stricture of the ureter in 90 % [89].

Ureteral strictures can be asymptomatic until graft dysfunction is discovered, or may be discovered by routine imaging. Hydronephrosis is most readily diagnosed by ultrasound but can be seen at CT, nuclear scintigraphy, and MRI. Ultrasound is excellent for the diagnosis of hydronephrosis where the dilated urine filled renal pelvis and calyces displace the echogenic sinus fat (Fig. 32.15a). Branching dilated calyces help to distinguish this entity from sinus cysts. The normal transplant ureter is not usually visible; when dilated, it will appear as a fluid-filled tubular structure between the renal pelvis and the bladder (Fig. 32.15b). Infection or rejection may cause thickening of the uroepithelium. Dilatation does not always signify obstruction however and may be secondary to vesico-ureteral reflux, a flaccid collecting system, an extrarenal pelvis, or a persistently dilated system post-obstruction or infection. Measurement of renovascular impedance using the resistive or pulsatility index has not proven useful in distinguishing obstruction from non-obstructive dilatation [2, 90]. Correlation with serum creatinine and urine output is valuable. Confirmation of obstruction can be achieved with technetium 99m MAG3 studies and a diuretic challenge; however, poor renal function will affect study validity [27]. Ureteral strictures are confirmed with CT or fluoroscopic nephrostography after obtaining catheter access to the collecting system (Fig. 32.15c, d). Confirmed ureteral obstruction can be drained by a percutaneous nephrostomy pending definitive management with balloon angioplasty, stent, or surgery (Fig. 32.15e).

Echoes and debris within the collecting system may represent blood clot, fungus, proteinaceous material, or infected debris. Gas may reflux into the collecting system from Foley catheterization of the bladder. Rarely, emphysematous pyelonephritis may produce gas throughout the renal parenchyma.

Urinary leak is an early complication occurring in 2 % [59]. Presenting features include rising creatinine, decreasing urine output, pain and swelling over the allograft or in the ipsilateral lower limb, increasing ascites, and fluid leakage from wound. Imaging will show a nonspecific fluid collection which can be aspirated for confirmation. Other than needle sampling, confirmation of a urine leak can be achieved with an isotope renogram, water-soluble contrast fluoroscopic cystogram or CT cystogram. The latter two have the advantage of directly demonstrating the location of the leak (Fig. 32.16a–c). Leaks are treated promptly because of risk of infection in the immunosuppressed host. Management depends upon the location of the leak [32]. Bladder or distal ureteral leaks may be managed by prolonged bladder catheter drainage or surgical repair whereas more proximal leaks may be treated by percutaneous nephrostomy or ureteral stenting pending definitive open repair [28, 32].

Urinary calculi are uncommon, occurring in 0.17–3 % of renal transplants [87]. These may occur de novo or be transplanted with the allograft and may present with acute obstruction, elevated creatinine, or infection. Stones in the native kidneys may also be a source of problems such as renal colic and infection after transplantation. Preoperative or intraoperative imaging can detect stones and prevent accidental stone transplantation. Calculi are readily diagnosed by ultrasound or CT, although small stones may be occult at ultrasound (Fig. 32.17a, b). Management depends on stone size.

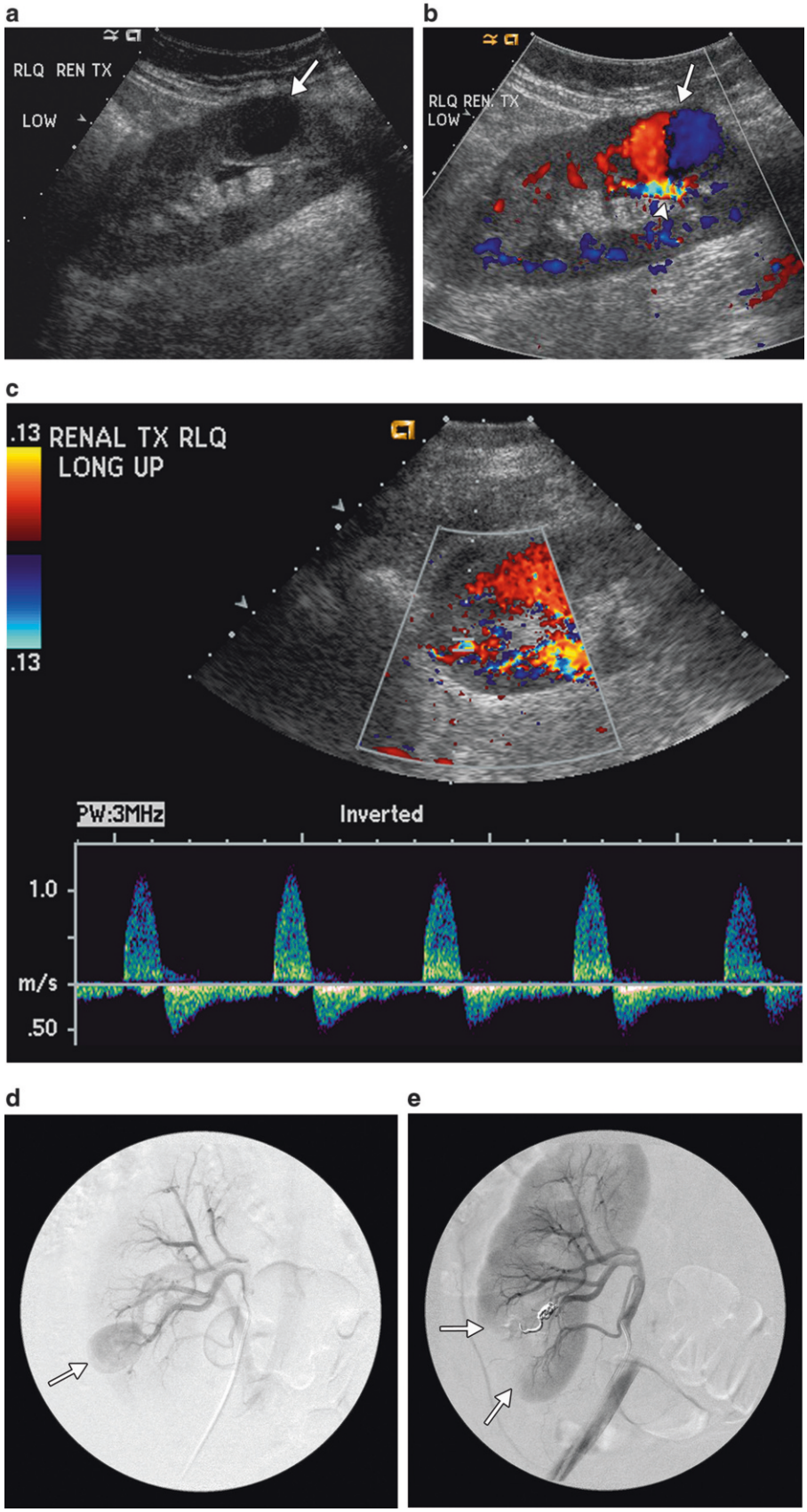

Fig. 32.14 Pseudoaneurysm. (**a**) Gray scale ultrasound shows an anechoic round structure in the lower pole (*arrow*). (**b**) Color Doppler reveals the vascular nature with internal yin yang swirling flow (*arrow*) and aliasing at the neck (*arrowhead*). (**c**) Duplex Doppler of the neck of a pseudoaneurysm demonstrating to and fro flow. (**d**) Selective digital subtraction catheter angiography shows opacification of a larger lower pole pseudoaneurysm (*arrow*). (**e**) Catheter angiography shows successful embolization with coils, with wedge-shaped perfusion defect (*arrows*)

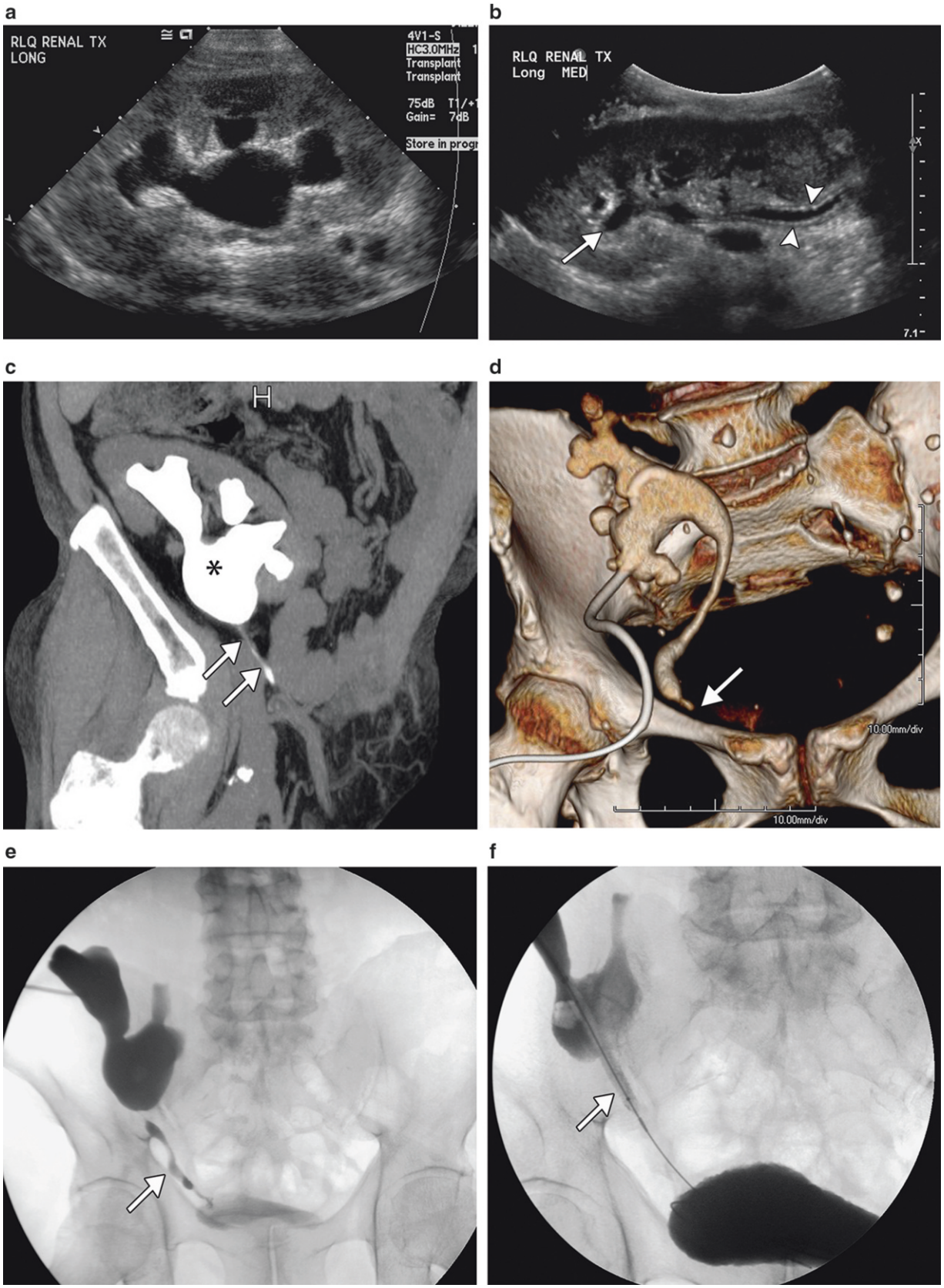

Fig. 32.15 (**a**) Gray scale ultrasound shows fluid within dilated calyces and renal pelvis. (**b**) Longitudinal gray scale image along the course of a ureter shows hydroureter with wall thickening (*arrowheads*) and mild hydronephrosis (*arrow*). (**c**) CT nephrostogram showing diffuse ureteral narrowing (*arrow*) and severe hydronephrosis (*asterisk*) (**d**) 3D volume rendered reconstruction shows the obstructed ureter (*arrow*) (**e/f**) Conventional nephrostogram performed before (**d**) and during (**e**) balloon dilatation (*arrow*) of the ureteral stricture

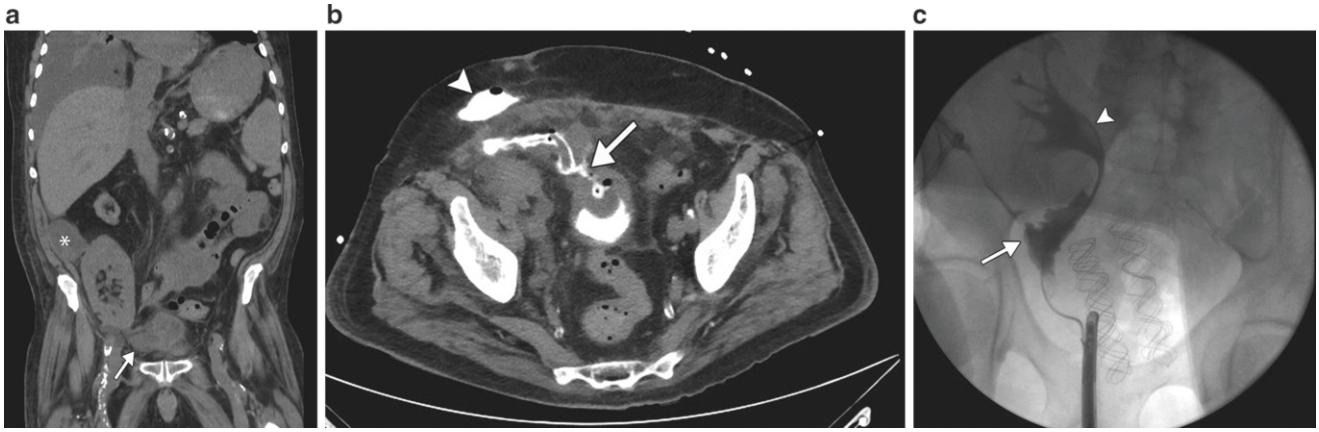

Fig. 32.16 Urinary leak. (**a**) Unenhanced coronal CT shows a fluid collection superolateral (*asterisk*) and a smaller collection medial (*arrow*) to the renal transplant. (**b**) Axial image during CT cystogram shows leakage of contrast from the bladder (*arrow*) into the right pelvis and anterior abdominal wall (*arrowhead*). (**c**) Conventional cystogram/retrograde ureterogram shows a leak (*arrow*). The transplant collecting system (*arrowhead*) is not dilated

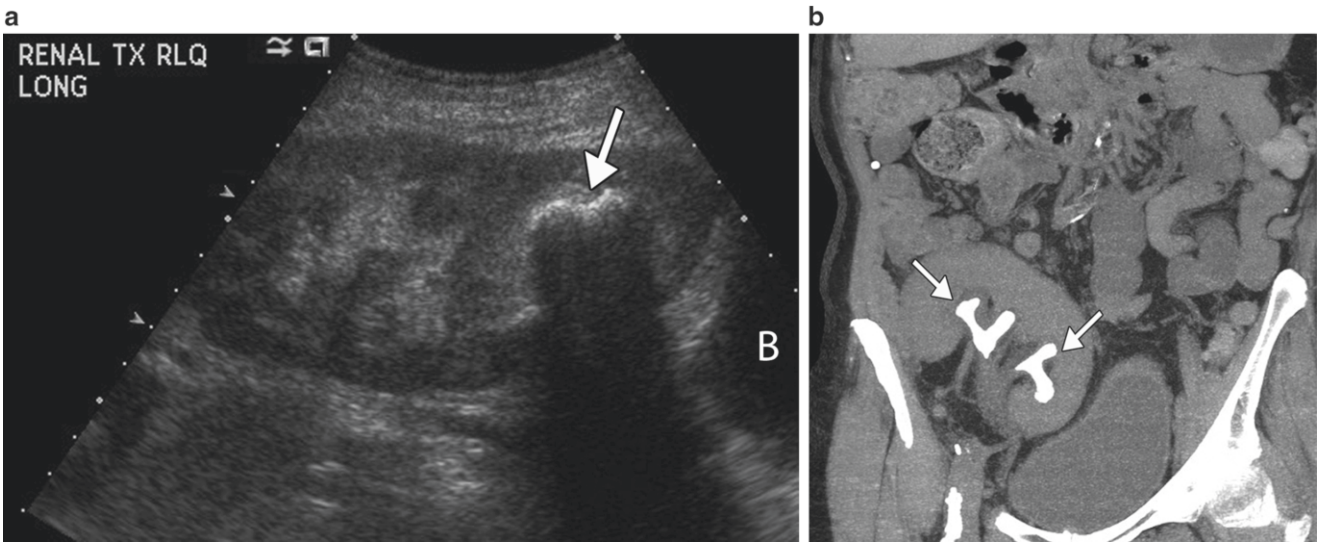

Fig. 32.17 Calculus. (**a**) Longitudinal gray scale ultrasound showing a lower pole calculus (*arrow*). The calculus is echogenic and causes posterior acoustic shadowing. Bladder (*B*). (**b**) Coronal CT shows a branched calculus in the upper and lower calyces of a right lower quadrant transplant (*arrows*)

Fluid Collections

Perigraft fluid collections may represent seromas, hematomas, lymphoceles, abscesses, and urinomas. Seromas, hematomas, and urinomas develop earlier than lymphoceles. Lymphoceles occur in 0.6–20 % of recipients overall, typically after 4 weeks, and are centered around the vascular pedicle of the allograft [59, 91]. Most fluid collections are asymptomatic but large collections can exert mass effect on the ureter, kidney, and vasculature with impairment of renal function. Infected collections may cause fever and pain. Fluid collections are easily detected by imaging with ultrasound, CT, and MRI (Fig. 32.18a, b). While time of onset and location may be diagnostically helpful, the appearance of the various collections (excluding hematoma) is similar. Imaging cannot diagnose an infected fluid collection unless it contains gas. Percutaneous aspiration (usually ultrasound guided) is necessary for microbiological evaluation and measurement of creatinine. Symptomatic lymphoceles can be managed by percutaneous drainage but they frequently recur. Further management options include percutaneous sclerotherapy and open or laparoscopic marsupialization [32]. Abscesses may be managed by percutaneous drains and antibiotics.

Most periallograft hematomas are contained in the pelvis, the appearance of hematoma varying depending on its age. Acute hematomas are hyperechoic and even solid appearing, potentially mistaken for pelvic fat or even bowel (Fig. 32.19a).

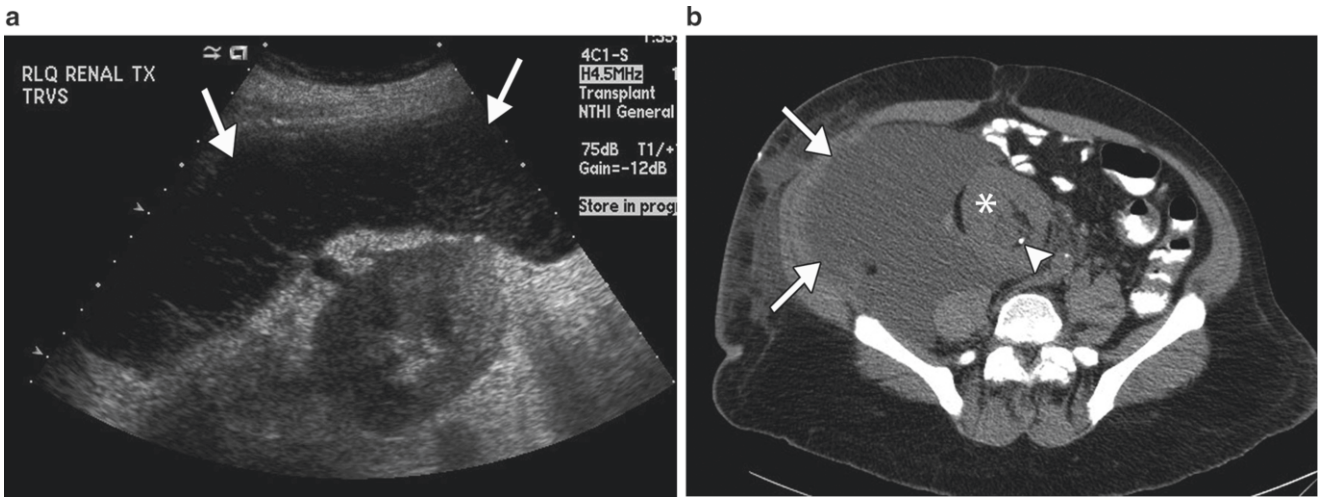

Fig. 32.18 Lymphocele. (**a**) Ultrasound shows a large complex fluid collection (*arrows*) displacing the transplant. (**b**) Computed tomography performed with oral contrast only. There is a large fluid collection (*arrows*) displacing the renal transplant (*asterisk*). A stent is seen within the renal pelvis (*arrowhead*)

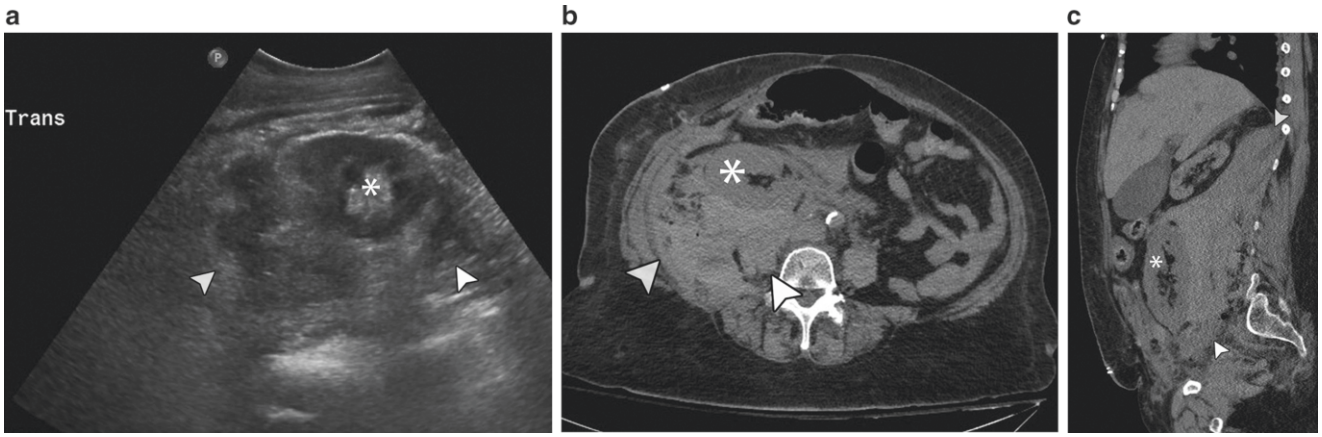

Fig. 32.19 Hematoma. (**a**) Ultrasound shows a complex perinephric hematoma (*arrowheads*) surrounding the transplant (*asterisk*). Axial (**b**) and sagittal (**c**) CT performed without oral or intravenous contrast shows higher density hematoma (*arrowhead*) in the retroperitoneum, displacing the renal transplant (*asterisk*) anteriorly

With degradation of blood products, hematomas become more cystic with internal fine septations or may be entirely anechoic. Free intraperitoneal hemorrhage is less common but readily detectable by sonography. Deep retroperitoneal or pelvic hematomas however may be missed by ultrasound. CT is a more sensitive imaging modality and can be performed immediately without any oral contrast. Acute hemorrhage is hyperattenuating on unenhanced CT (Fig. 32.19b, c). While MR is not indicated for hemorrhage, acute hematoma has high signal intensity on T1-weighted images and is more variable on T2-weighted images.

Infection

Infection in the allograft is diagnosed by urine and blood cultures. Imaging findings are nonspecific and include graft swelling, urothelial thickening, altered perfusion, and hydronephrosis with debris. Parenchymal abscesses are rounded fluid collections with a thick wall and internal debris. They may be aspirated under ultrasound guidance for diagnosis and treatment.

BKV infection is now recognized as a serious cause of graft loss [92–94]. Up to 8 % of recipients develop BKV-associated nephropathy with a graft loss rate of up to 40–50 % [93, 94]. BKV infection can be detected and monitored with serum and urine viral DNA. Imaging has a limited role in the diagnosis of BKV nephropathy. However ureteral stricture and hydronephrosis have been reported [95]. Ultrasound may be used to guide allograft biopsy for histologic confirmation.

The role of imaging in other infections depends on the target organ. CT is useful for screening the patient with fever and leukocytosis. Gastrointestinal or infectious disease such as colitis, diverticulitis, pneumonia, or intra-abdominal

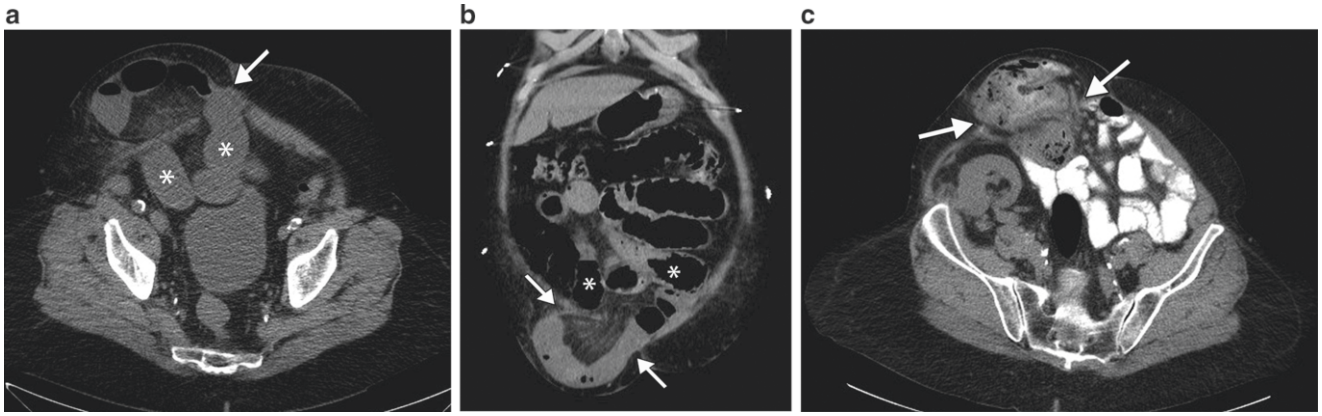

Fig. 32.20 Incisional hernia. Axial CT shows dilated small bowel (*asterisk*) secondary to an incisional hernia (*arrow*). (**a/b**) Axial (**a**) and coronal (**b**) CT without oral contrast shows dilated small bowel loops (*asterisk*) secondary to an incisional hernia (*arrows*). (**c**) Axial CT with oral contrast shows small bowel loops herniating through the incisional defect (*arrows*), without causing small bowel obstruction

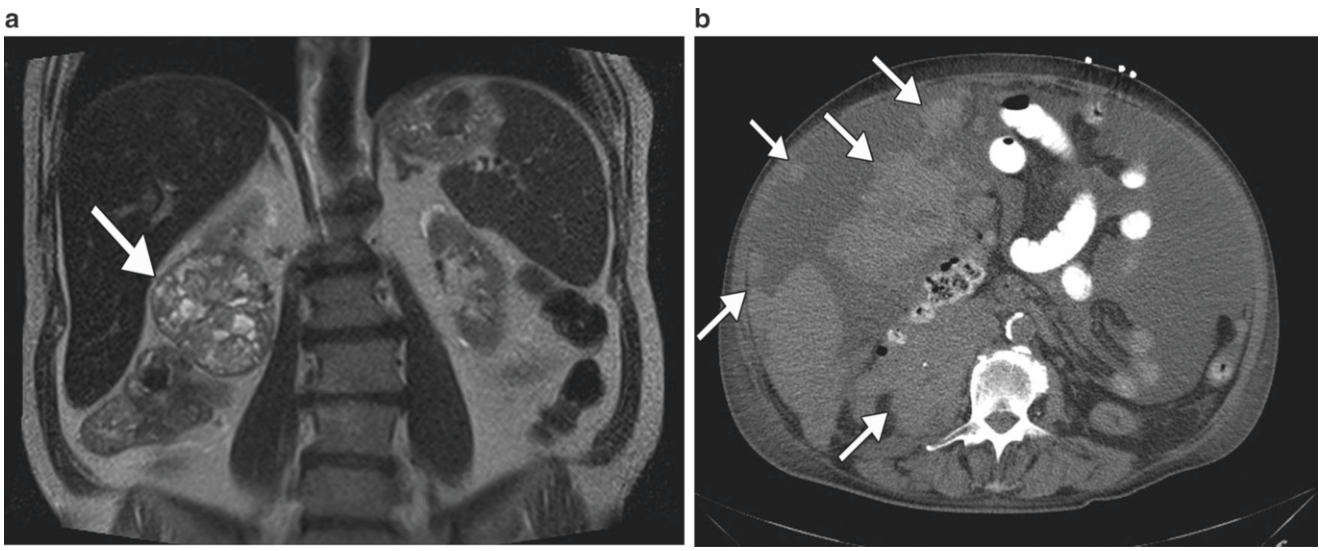

Fig. 32.21 Renal cell carcinoma. (**a**) Coronal T2-weighted MR shows a mixed solid and cystic mass in the lower pole of the native right kidney (*arrow*). Note the atrophic left kidney. (**b**) Following right nephrectomy, the patient developed extensive metastatic disease throughout the peritoneal cavity and right renal fossa (*arrows*) demonstrated by CT

infection may be found. Wound-related complications such as infection (1 %) and hernia or dehiscence (1.5 %) can be diagnosed with CT or US (Fig. 32.20) [59].

Post-transplant Malignancy

Between 6 and 20 % of recipients develop cancer after 10 years, the most common being skin (95 % are nonmelanoma, mainly squamous cell). There is also a twofold increased risk of non-skin malignancy after solid organ transplantation due to immunosuppression [96–98]. Mortality is high (up to 50 %) [96, 99]. Cancers may arise de novo in the recipient, may be recurrent in the recipient, or may be transmitted from the donor. Virus-induced malignancies such as lymphoma, Kaposi sarcoma, and anogenital and liver cancer are increased 3–50 times [99, 100]. Imaging findings may not be specific but image-guided biopsy may provide the diagnosis.

Renal cell carcinoma is more common in native kidneys of renal transplant recipients and the second most common malignancy after transplantation (Fig. 32.21) [98]. Early cases may result from malignant transformation in cysts associated with end stage kidneys and hemodialysis [99]. However renal carcinoma in native kidneys may develop in the absence of acquired cystic disease [101]. Clear cell subtype is slightly more common than papillary carcinoma and the prognosis is good [102]. Native renal cell carcinoma tends to be bilateral, multifocal, and less aggressive and can be treated with partial or total nephrectomy [103]. Renal carcinoma can also occur in the allograft, with papillary carcinoma being more common [102].

Many of these tumors are detected incidentally at imaging. Ultrasound is generally the first-line modality for the allograft but is less sensitive in the evaluation of the native kidneys which may be atrophic and/or replaced by cysts.

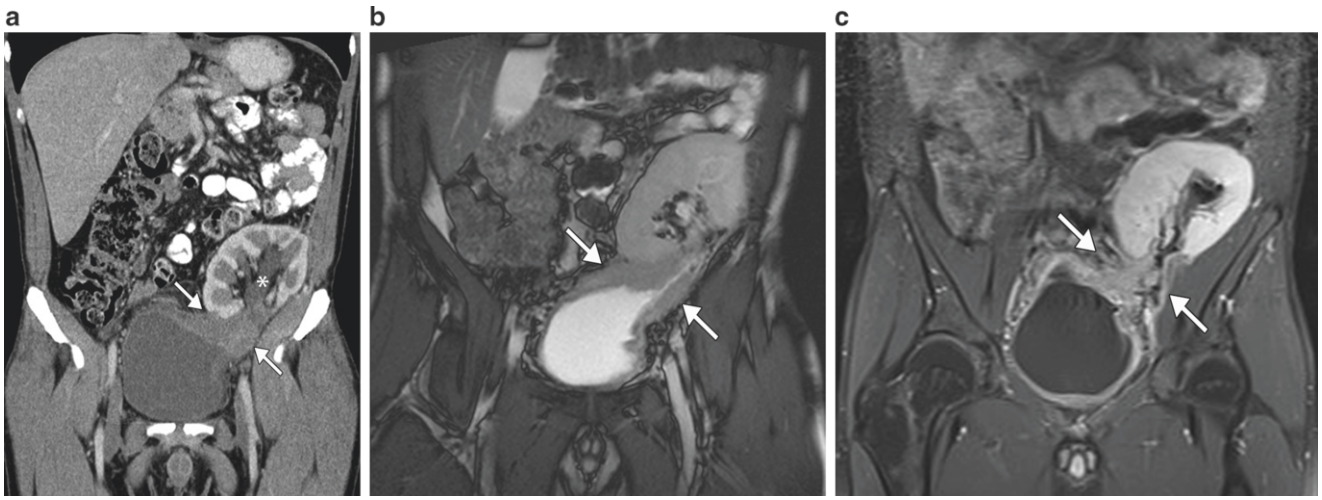

Fig. 32.22 Urothelial carcinoma in a 37-year-old man with a history of reflux nephropathy presenting with hematuria 6 years after cadaveric renal transplant. (**a**) Enhanced CT shows infiltrating tumor (*arrows*) at the bladder dome extending superiorly and encasing the ureter. There is hydronephrosis (*asterisk*). (**b**) Coronal T2-weighted image better shows the irregular bladder wall thickening extending superiorly to encase the transplanted ureter (*arrows*). (**c**) Enhanced MR shows avid enhancement of the tumor, with infiltration of the surrounding fat (*arrows*)

More comprehensive evaluation and staging is provided by CT or MR performed with intravenous contrast (Fig. 32.21). Renal carcinoma is typically a mass with no fatty component in which enhancement (a surrogate for neovascularity) occurs after intravenous contrast, imaged by CT, MRI, or contrast-enhanced ultrasound [104–107]. Necrosis, calcification, hemorrhage, and cystic components all contribute to tumor heterogeneity at imaging. In contrast to clear cell RCC, papillary renal carcinoma is typically smaller, more homogenous, and enhances less [108]. However cystic variants may occur. Comprehensive staging is multimodality based and includes MRI and PET–CT.

Urothelial bladder cancer may be as common as renal carcinoma in some series. It occurs in younger patients and has a more aggressive course [109] (Fig. 32.22).

Post-transplant Lymphoproliferative Disorder

Post-transplant lymphoproliferative disorder (PTLD) is a spectrum of disease related to transmission of Epstein–Barr virus (EBV) in 90 % of cases. Around 1 % of renal recipients develop PTLD, usually within the first year [110]. However PTLD can occur at any time, with a median time of onset of 5 years [110]. PTLD may be nodal or extra-nodal. In renal transplant recipients, extra-nodal disease is more common and the allograft is involved in 10 % [110]. Any solid or hollow viscera (liver, spleen, lung, bowel, bone marrow) can be involved by single or multiple masses [110]. Presenting features are nonspecific, and can include fever, weight loss, lymphadenopathy, or declining renal function. Incidental discovery at imaging is not unusual. Imaging findings are not specific, and can mimic lymphoma, metastasis, or infection. There may be focal or diffuse involvement of organs and bowel. Soft tissue masses at the renal transplant hilum are very suggestive [111, 112]. These tend to be hypoechoic at ultrasound with internal vascularity and causing hydronephrosis. At MRI, the low T2 signal intensity of the renal hilar mass and poor enhancement is characteristic [111]. Pathological diagnosis is necessary and can be achieved with ultrasound or CT-guided biopsy depending upon location. CT and FDG PET/CT are useful for diagnosis, staging, and follow-up (Fig. 32.23).

Summary

This chapter has attempted to familiarize the renal physician or surgeon with the role of imaging in the management of renal transplantation. The wide range of post-transplant complications is difficult to evaluate and distinguish on clinical and laboratory examination. This review provides guidance regarding the role of various radiologic modalities in early and accurate diagnosis and the contribution of percutaneous interventional techniques to patient management. While imaging is currently of limited value in the diagnosis of parenchymal disorders such as acute rejection, the ability to exclude other causes of transplant dysfunction is still valuable. In the future, noninvasive imaging tools may reduce the need for transplant biopsy.

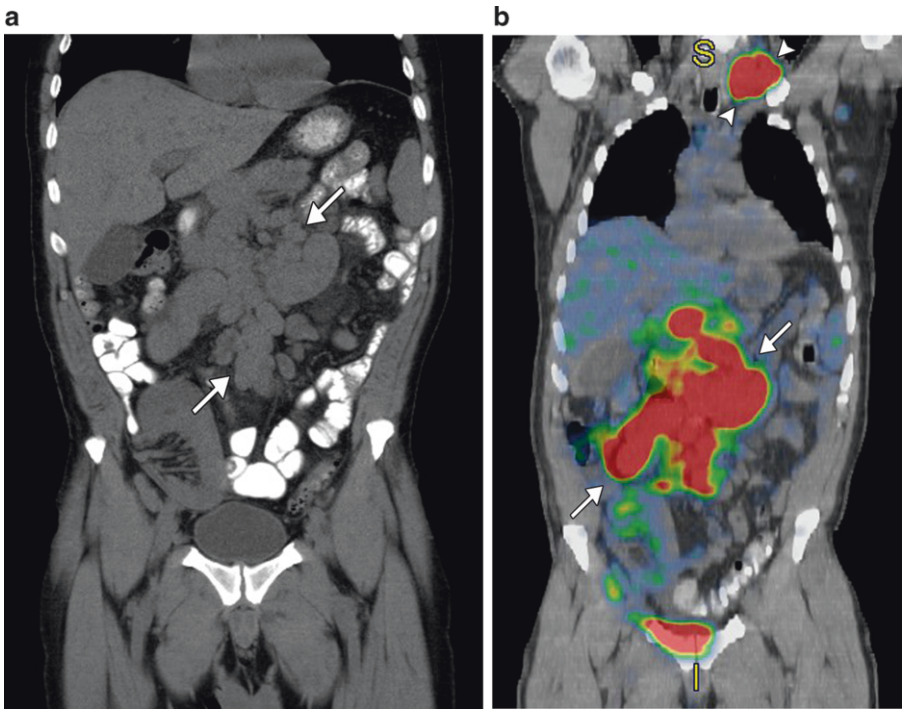

Fig. 32.23 B cell lymphoma in a 65-year-old, 5 years after renal transplant. (**a**) Unenhanced coronal CT shows multiple enlarged lymph nodes (*arrows*) in the mesentery. The renal transplant is not involved. (**b**) CT/PET fusion shows abnormal metabolic activity in the mesenteric lymph nodes (*arrows*) as well as left cervical lymph nodes (*arrowheads*)

Key Points

1. Imaging plays a key role in the pre- and postoperative evaluation of renal transplantation.
2. Ultrasound imaging is most useful in the diagnosis of hydronephrosis, fluid collections, and vascular complications.
3. Imaging findings of rejection are nonspecific.
4. CTA and MRA are useful for confirmation of vascular complications prior to intervention.

References

1. Khosroshahi HT, Tarzamni M, Oskuii RA. Doppler ultrasonography before and 6 to 12 months after kidney transplantation. Transplant Proc. 2005;37(7):2976–81. PubMed PMID: 16213279.
2. Cosgrove DO, Chan KE. Renal transplants: what ultrasound can and cannot do. Ultrasound Q. 2008;24(2):77–87; quiz 141–2. PubMed PMID: 18528243.
3. Baxter GM. Ultrasound of renal transplantation. Clin Radiol. 2001;56:802–18.
4. Khosroshahi HT, Heris HK, Makhdami N, Habibzadeh A, Badrogli N, Oskoii R, Jahannavard N. Time-dependent Doppler ultrasonographic findings in transplanted kidneys from living donors: a 5-year follow-up study. Transplant Proc. 2011;43(2):482–4. PubMed PMID: 21440739.
5. Quarto Di Palo F, Rivolta R, Elli A, et al. Relevance of resistive index ultrasonographic measurement in renal transplantation. Nepron. 1996;73:195–200.
6. Gao J, Rubin JM, Xiang DY, He W, Auh YH, Wang J, Ng A, Min R. Doppler parameters in renal transplant dysfunction: correlations with histopathologic changes. J Ultrasound Med. 2011;30(2):169–75. PubMed PMID: 21266554.
7. Radermacher J, Mengel M, Ellis S, et al. The renal arterial resistance index and renal allograft survival. N Engl J Med. 2003;349:115–24.
8. McArthur C, Baxter GM. Current potential renal applications of contrast-enhanced ultrasound. Clin Radiol. 2012;67(9):909–22. Epub 2012 Mar 30.
9. Grzelak P, Szymczyk K, Strzelczyk J, et al. Perfusion of kidney graft pyramids and cortex in contrast-enhanced ultrasonography in the determination of the cause of delayed graft function. Ann Transplant. 2011;23(16):48–53.
10. Ahuja TS, Niaz N, Agraharkar M. Contrast-induced nephrotoxicity in renal allograft recipients. Clin Nephrol. 2000;54:11–4.
11. Katzberg RW, Newhouse JH. Intravenous contrast medium-induced nephrotoxicity: is the medical risk really as great as we have come to believe? Radiology. 2010;256(1):21–8. PubMed PMID: 20574082.
12. Tonolini M, Bianco R. Multidetector CT cystography for imaging colovesical fistulas and iatrogenic bladder leaks. Insights Imaging. 2012;3(2):181–7. Epub 2012 Feb 4. PubMed PMID: 22696044; PubMed Central PMCID: PMC3314733.
13. Chan DP, Abujudeh HH, Cushing Jr GL, Novelline RA. CT cystography with multiplanar reformation for suspected bladder rupture: experience in 234 cases. AJR Am J Roentgenol. 2006;187(5):1296–302. PubMed PMID: 17056919.

14. Titton RL, Gervais DA, Hahn PF, Harisinghani MG, Arellano RS, Mueller PR. Urine leaks and urinomas: diagnosis and imaging-guided intervention. Radiographics. 2003;23(5):1133–47. PubMed PMID: 12975505.
15. Ismaeel MM, Abdel-Hamid A. Role of high resolution contrast-enhanced magnetic resonance angiography (HR CeMRA) in management of arterial complications of the renal transplant. Eur J Radiol. 2011;79(2):e122–7. Epub 2011 May 20. PubMed PMID: 21601400.
16. Lanzman RS, Voiculescu A, Walther C, Ringelstein A, Bi X, Schmitt P, Freitag SM, Won S, Scherer A, Blondin D. ECG-gated nonenhanced 3D steady-state free precession MR angiography in assessment of transplant renal arteries: comparison with DSA. Radiology. 2009;252(3):914–21. PubMed PMID: 19635833.
17. Liu X, Berg N, Sheehan J, Bi X, Weale P, Jerecic R, Carr J. Renal transplant: nonenhanced renal MR angiography with magnetization-prepared steady-state free precession. Radiology. 2009;251(2):535–42. Epub 2009 Mar 4. PubMed PMID: 19261926.
18. Wang Y, Alkasab TK, Narin O, Nazarian RM, Kaewlai R, Kay J, Abujudeh HH. Incidence of nephrogenic systemic fibrosis after adoption of restrictive gadolinium-based contrast agent guidelines. Radiology. 2011;260(1):105–11. Epub 2011 May 17. PubMed PMID: 21586680.
19. Michaely HJ, Herrmann KA, Nael K, Oesingmann N, Reiser MF, Schoenberg SO. Functional renal imaging: nonvascular renal disease. Abdom Imaging. 2007;32(1):1–16. Epub 2006 Jan 30. PubMed PMID: 16447077.
20. Sadowski EA, Djamali A, Wentland AL, Muehrer R, Becker BN, Grist TM, Fain SB. Blood oxygen level-dependent and perfusion magnetic resonance imaging: detecting differences in oxygen bioavailability and blood flow in transplanted kidneys. Magn Reson Imaging. 2010;28(1):56–64. Epub 2009 Jul 3. PubMed PMID: 19577402; PubMed Central PMCID: PMC2891158.
21. Palmucci S, Mauro LA, Veroux P, Failla G, Milone P, Ettorre GC, Sinagra N, Giuffrida G, Zerbo D, Veroux M. Magnetic resonance with diffusion-weighted imaging in the evaluation of transplanted kidneys: preliminary findings. Transplant Proc. 2011;43(4):960–6. PubMed PMID: 21620026.
22. Artz NS, Sadowski EA, Wentland AL, Grist TM, Seo S, Djamali A, Fain SB. Arterial spin labeling MRI for assessment of perfusion in native and transplanted kidneys. Magn Reson Imaging. 2011;29(1):74–82. Epub 2010 Sep 17. PubMed PMID: 20850241; PubMed Central PMCID: PMC3005910.
23. Lee CU, Glockner JF, Glaser KJ, Yin M, Chen J, Kawashima A, Kim B, Kremers WK, Ehman RL, Gloor JM. MR elastography in renal transplant patients and correlation with renal allograft biopsy: a feasibility study. Acad Radiol. 2012;19(7):834–41. Epub 2012 Apr 13. PubMed PMID: 22503893; PubMed Central PMCID: PMC3377786.
24. Bonekamp S, Corona-Villalobos CP, Kamel IR. Oncologic applications of diffusion-weighted MRI in the body. J Magn Reson Imaging. 2012;35(2):257–79. doi:10.1002/jmri.22786. PubMed PMID: 22271274.
25. Hohenwalter MD, Skowlund CJ, Erickson SJ, et al. Renal transplant evaluation with MR angiography and MR imaging. Radiographics. 2001;21:1505–17.
26. Jain R, Sawhney S. Contrast-enhanced MR angiography (CE-MRA) in the evaluation of vascular complications of renal transplantation. Clin Radiol. 2005;60(11):1171–81. PubMed PMID: 16223613.
27. El-Maghraby TA, de Fijter JW, van Eck-Smit BL, Zwinderman AH, El-Haddad SI, Pauwels EK. Renographic indices for evaluation of changes in graft function. Eur J Nucl Med. 1998;25(11):1575–86. PubMed PMID: 9799356.
28. Hobart MG, Streem SB, Gill IS. Renal transplant complications: minimally invasive management. Urol Clin North Am. 2000;27:787–98.
29. Sandhu C, Patel U. Renal transplant dysfunction: the role of interventional radiology. Clin Radiol. 2002;57:772–83.
30. Kim HS, Fine DM, Atta MG. Catheter-directed thrombectomy and thrombolysis for acute renal vein thrombosis. J Vasc Interv Radiol. 2006;17(5):815–22. PubMed PMID: 16687747.
31. Melamed ML, Kim HS, Jaar BG, Molmenti E, Atta MG, Samaniego MD. Combined percutaneous mechanical and chemical thrombectomy for renal vein thrombosis in kidney transplant recipients. Am J Transplant. 2005;5(3):621–6. PubMed PMID: 15707419.
32. Kobayashi K, Censullo ML, Rossman LL, Kyriakides PN, Kahan BD, Cohen AM. Interventional radiologic management of renal transplant dysfunction: indications, limitations, and technical considerations. Radiographics. 2007;27(4):1109–30. PubMed PMID: 17620470.
33. Nicolini A, Ferraresso M, Lovaria M, et al. Carbon dioxide subtraction angiography for management of kidney transplant vascular complications. Transplant Proc. 2001;33:3388–9.
34. Moresco KP, Patel NH, Namyslowski Y, et al. Carbon dioxide angiography of the transplanted kidney: technical considerations and imaging findings. Am J Roentgenol. 1998;171:1271–6.
35. Beecroft JR, Rajan DK, Clark TW, Robinette M, Stavropoulos SW. Transplant renal artery stenosis: outcome after percutaneous intervention. J Vasc Interv Radiol. 2004;15(12):1407–13. PubMed PMID: 15590798.
36. Valpreda S, Messina M, Rabbia C. Stenting of transplant renal artery stenosis: outcome in a single center study. J Cardiovasc Surg (Torino). 2008;49(5):565–70. PubMed PMID: 18670375.
37. Marini M, Fernandez-Rivera C, Cao I, Gulias D, Alonso A, Lopez-Muñiz A, Gómez-Martínez P. Treatment of transplant renal artery stenosis by percutaneous transluminal angioplasty and/or stenting: study in 63 patients in a single institution. Transplant Proc. 2011;43(6):2205–7. PubMed PMID: 21839234.
38. Pham PT, Pham PA, Pham PC, Parikh S, Danovitch G. Evaluation of adult kidney transplant candidates. Semin Dial. 2010;23(6):595–605. doi:10.1111/j.1525-139X.2010.00809.x. PubMed PMID: 21175834.
39. Catalá V, Martí T, Diaz JM, Cordeiro E, Samaniego J, Rosales A, De La Torre P. Use of multidetector CT in presurgical evaluation of potential kidney transplant recipients. Radiographics. 2010;30(2):517–31. PubMed PMID: 20228332.
40. Koc F, Ozdemir K, Kaya MG, Dogdu O, Vatankulu MA, Ayhan S, Erkorkmaz U, Sonmez O, Aygul MU, Kalay N, Kayrak M, Karabag T, Alihanoglu Y, Gunebakmaz O. Intravenous N-acetylcysteine plus high-dose hydration versus high-dose hydration and standard hydration for the prevention of contrast-induced nephropathy: CASIS–a multicenter prospective controlled trial. Int J Cardiol. 2012;155(3):418–23. Epub 2010 Nov 23. PubMed PMID: 21106264.
41. Calabrò P, Bianchi R, Crisci M, Caprile M, Bigazzi MC, Palmieri R, Golia E, De Vita A, Romano IJ, Limongelli G, Russo MG, Calabrò R. Use and efficacy of saline hydration and N-acetyl cysteine to prevent contrast-induced nephropathy in low-risk populations undergoing coronary artery angiography. Intern Emerg Med. 2011;6(6):503–7. Epub 2011 Jan 29. PubMed PMID: 21279477.
42. Bader BD, Berger ED, Heede MB, Silberbaur I, Duda S, Risler T, Erley CM. What is the best hydration regimen to prevent contrast media-induced nephrotoxicity? Clin Nephrol. 2004;62(1):1–7. PubMed PMID: 15267006.
43. Smith D, Chudgar A, Daly B, Cooper M. Evaluation of potential renal transplant recipients with computed tomography angiography. Arch Surg. 2012;147(12):1114–22. doi:10.1001/archsurg.2012.1466. PubMed PMID: 23248013.
44. Maisonneuve P, Agodoa L, Gellert R, Stewart JH, Buccianti G, Lowenfels AB, Wolfe RA, Jones E, Disney AP, Briggs D, McCredie M, Boyle P. Cancer in patients on dialysis for end-stage renal disease: an international collaborative study. Lancet. 1999;354(9173):93–9. PubMed PMID: 10408483.

45. Park SB, Kim JK, Cho KS. Complications of renal transplantation: ultrasonographic evaluation. J Ultrasound Med. 2007;26(5):615–33. PubMed PMID: 17460004.
46. Jones JW, Hunter DW, Matas AJ. Post transplant lymphoceles: a critical look into the risk factors, pathophysiology and management. J Urol. 1993;150:22–6.
47. Linkowski GD, Warvariv V, Filly RA, et al. Sonography in the diagnosis of acute renal allograft rejection and cyclosporin toxicity. Am J Roentgenol. 1987;148:291–5.
48. Kelcz F, Pozniak MA, Pirsch JD, Oberly TD. Pyramidal appearance and resistive index: insensitive and nonspecific sonographic indicators of renal transplant rejection. Am J Roentgenol. 1990;155:531–5.
49. Don S, Kopecky KK, Filo RS, et al. Duplex Doppler US of renal allografts: causes of elevated resistive index. Radiology. 1989; 171:709–12.
50. Genkins SM, Sanfillippo FP, Carroll BA. Duplex Doppler sonography of renal transplants: lack of sensitivity and specificity in establishing pathologic diagnosis. Am J Roentgenol. 1989;152:535–9.
51. Grant EG, Perrella RR. Wishing won't make it so: duplex Doppler sonography in the evaluation of renal transplant dysfunction. Am J Roentgenol. 1990;155:538–9.
52. Perchik JE, Baumgartner BR, Bernardino ME. Renal transplant rejection. Limited value of duplex Doppler sonography. Invest Radiol. 1991;26:422–6.
53. Fischer T, Filimonow S, Dieckhöfer J, et al. Improved diagnosis of early kidney allograft dysfunction by ultrasound with echo enhancer–a new method for the diagnosis of renal perfusion. Nephrol Dial Transplant. 2006;21(10):2921–9. Epub 2006 Jul 5. PMID: 16822787.
54. Fischer T, Dieckhofer J, Muhler M, et al. The use of contrast-enhanced US in renal transplant: first results and potential clinical benefit. Eur Radiol. 2005;15 Suppl 5:E109–16. PMID: 18637238.
55. Clevert DA, D'Anastasi M, Jung EM. Contrast-enhanced ultrasound and microcirculation: efficiency through dynamics—current developments. Clin Hemorheol Microcirc. 2013;53:171–86. Epub ahead of print. PMID: 22986755.
56. Howard RJ, Patton PR, Reed AI, et al. The changing causes of graft loss and death after kidney transplantation. Transplantation. 2002;73:1923–8.
57. Shah A. Radionuclide imaging in organ transplantation. Radiol Clin North Am. 1995;33:473–96.
58. Kim EE, Pjura G, Lowry P, et al. Cyclosporin-A nephrotoxicity and acute cellular rejection in renal transplant recipients: correlation between radionuclide and histologic findings. Radiology. 1986;159:443–6.
59. Eufrásio P, Parada B, Moreira P, Nunes P, Bollini S, Figueiredo A, Mota A. Surgical complications in 2000 renal transplants. Transplant Proc. 2011;43(1):142–4.
60. Aktas S, Boyvat F, Sevmis S, Moray G, Karakayali H, Haberal M. Analysis of vascular complications after renal transplantation. Transplant Proc. 2011;43(2):557–61. PubMed PMID: 21440760.
61. Wong-You-Cheong JJ, Grumbach K, Krebs TL, Pace ME, Daly BD, Chow CC, Johnson LB, Bartlett ST. Torsion of intraperitoneal renal transplants: imaging appearances. Am J Roentgenol. 1998;171:1355–9.
62. Rouviere O, Berger P, Beziat C, et al. Acute thrombosis of renal transplant artery: graft salvage by means of intra-arterial fibrinolysis. Transplantation. 2002;73:403–9.
63. Reuther G, Wanjura D, Bauer H. Acute renal vein thrombosis in renal allografts: detection with duplex Doppler US. Radiology. 1989;170:557–8.
64. Kaveggia LP, Parrella RR, Grant EG, et al. Duplex Doppler sonography in renal allografts: the significance of reversed flow in diastole. Am J Roentgenol. 1990;155:295–8.
65. Takahashi M, Humke U, Girndt M, et al. Early posttransplantation renal allograft perfusion failure due to dissection: diagnosis and interventional treatment. Am J Roentgenol. 2003;180:759–63.
66. Tublin ME, Dodd III GD. Sonography of renal transplantation. Radiol Clin North Am. 1995;33:447–59.
67. Gufler H, Weimer W, Neu K, Wagner S, Rau WS. Contrast enhanced MR angiography with parallel imaging in the early period after renal transplantation. J Magn Reson Imaging. 2009;29(4):909–16. PubMed PMID: 19306426.
68. Jakobsen JA, Brabrand K, Egge TS, et al. Doppler examination of the allografted kidney. Acta Radiol. 2003;44:3–12.
69. Hurst FP, Abbott KC, Neff RT, Elster EA, Falta EM, Lentine KL, Agodoa LY, Jindal RM. Incidence, predictors and outcomes of transplant renal artery stenosis after kidney transplantation: analysis of USRDS. Am J Nephrol. 2009;30(5):459–67. Epub 2009 Sep 24. PubMed PMID: 19776559.
70. de Morais RH, Muglia V, Mamere AE, et al. Duplex Doppler sonography of transplant renal artery stenosis. J Clin Ultrasound. 2003;31:135–41.
71. Ardalan MR, Tarzamani MK, Shoja MM. A correlation between direct and indirect Doppler ultrasonographic measures in transplant renal artery stenosis. Transplant Proc. 2007;39(5):1436–8. PubMed PMID: 17580156.
72. Baxter GM, Ireland H, Moss JG, Harden PN, Junor BJ, Rodger RS, Briggs JD. Colour Doppler ultrasound in renal transplant artery stenosis: which Doppler index? Clin Radiol. 1995;50(9):618–22. PubMed PMID: 7554736.
73. Snider JF, Hunter DW, Muradian GP, et al. Transplant renal artery stenosis: evaluation with duplex sonography. Radiology. 1989;172:1027–30.
74. Patel U, Khaw KK, Hughes NC. Doppler ultrasound for detection of renal transplant artery stenosis-threshold peak systolic velocity needs to be higher in a low-risk or surveillance population. Clin Radiol. 2003;58(10):772–7. PubMed PMID: 14521886.
75. Gottlieb RH, Lieberman JL, Pabico RC, Waldman DL. Diagnosis of renal artery stenosis in transplanted kidneys: value of Doppler waveform analysis of the intrarenal arteries. AJR Am J Roentgenol. 1995;165(6):1441–6. PubMed PMID: 7484582.
76. Cook A, Khoury A, Kader K, Hebert D, Navarro O, Pippi-Salle J, Farhat W. Does peak systolic velocity correlate with renal artery stenosis in a pediatric renal transplant population? Pediatr Transplant. 2006;10(5):608–12. PubMed PMID:16856998.
77. Glockner JF, Takahashi N, Kawashima A, Woodrum DA, Stanley DW, Takei N, Miyoshi M, Sun W. Non-contrast renal artery MRA using an inflow inversion recovery steady state free precession technique (Inhance): comparison with 3D contrast-enhanced MRA. J Magn Reson Imaging. 2010;31(6):1411–8. PubMed PMID: 20512894.
78. Utsunomiya D, Miyazaki M, Nomitsu Y, Komeda Y, Okigawa T, Urata J, Yamashita Y. Clinical role of non-contrast magnetic resonance angiography for evaluation of renal artery stenosis. Circ J. 2008;72(10):1627–30. Epub 2008 Aug 27. PubMed PMID: 18728334.
79. Serai S, Towbin AJ, Podberesky DJ. Non-contrast MRA using an inflow-enhanced, inversion recovery SSFP technique in pediatric abdominal imaging. Pediatr Radiol. 2012;42(3):364–8. Epub 2011 Nov 10. PubMed PMID: 22072071.
80. Heer MK, Trevillian PR, Hardy DB, Hibberd AD. Salvaging kidneys with renal allograft compartment syndrome. Transpl Int. 2012;25(4):e47–9. doi:10.1111/j.1432-2277.2012.01442.x. Epub 2012 Feb 6. PubMed PMID: 22309228.
81. Ball CG, Kirkpatrick AW, Yilmaz S, Monroy M, Nicolaou S, Salazar A. Renal allograft compartment syndrome: an underappreciated postoperative complication. Am J Surg. 2006;191(5):619–24. PubMed PMID: 16647348.
82. Middleton WDE, Bellman GM, Melon GL, et al. Post-biopsy renal transplant arteriovenous fistulas: color Doppler ultrasound characteristics. Radiology. 1989;171:253–7.
83. Loffroy R, Guiu B, Lambert A, Mousson C, Tanter Y, Martin L, Cercueil JP, Krausé D. Management of post-biopsy renal allograft arteriovenous fistulas with selective arterial embolization: immediate

and long-term outcomes. Clin Radiol. 2008;63(6):657–65. Epub 2008 Feb 20. PubMed PMID: 18455557.
84. Pine J, Rajaganeshan R, Baker R, Lewington A, Patel J, Menon K, Kessel D, Ahmad N. Early postoperative renal vein stenosis after renal transplantation: a report of two cases. J Vasc Interv Radiol. 2010;21(2):303–4. PubMed PMID: 20123217.
85. Streeter EH, Little DM, Cranston DW, et al. The urological complications of renal transplantation: a series of 1535 patients. BJU Int. 2002;90:627–34.
86. Fayek SA, Keenan J, Haririan A, Cooper M, Barth RN, Schweitzer E, Bromberg JS, Bartlett ST, Philosophe B. Ureteral stents are associated with reduced risk of ureteral complications after kidney transplantation: a large single center experience. Transplantation. 2012;93(3):304–8. PubMed PMID: 22179401.
87. Sackett DD, Singh P, Lallas CD. Urological involvement in renal transplantation. Int J Urol. 2011;18(3):185–93.
88. Faenza A, Nardo B, Catena F, et al. Ureteral stenosis after kidney transplantation. Transpl Int. 1999;12:334–40.
89. Berger PM, Diamond JR. Ureteral obstruction as complication of renal transplantation: a review. J Nephrol. 1998;11:20–3.
90. Salgado OJ, Martin MG, Urdaneta B, et al. Serial pulsatility index measurements in renal grafts before, during and after episodes of urinary obstruction. J Ultrasound Med. 1999;18:827–30.
91. Zagdoun E, Ficheux M, Lobbedez T, Chatelet V, Thuillier-Lecouf A, Bensadoun H, Ryckelynck JP, Hurault de Ligny B. Complicated lymphoceles after kidney transplantation. Transplant Proc. 2010;42(10):4322–5. PubMed PMID: 21168691.
92. Ramos E, Drachenberg CB, Papadimitriou JC, et al. Clinical course of polyoma virus nephropathy in 67 renal transplant patients. J Am Soc Nephrol. 2002;13:2145–51.
93. Cannon RM, Ouseph R, Jones CM, Hughes MG, Eng M, Marvin MR. BK viral disease in renal transplantation. Curr Opin Organ Transplant. 2011;16(6):576–9.
94. Dall A, Hariharan S. BK virus nephritis after renal transplantation. Clin J Am Soc Nephrol. 2008;3 Suppl 2:S68–75. PubMed PMID: 18309005; PubMed Central PMCID: PMC3152275.
95. Gupta M, Miller F, Nord EP, Wadhwa NK. Delayed renal allograft dysfunction and cystitis associated with human polyomavirus (BK) infection in a renal transplant recipient: a case report and review of literature. Clin Nephrol. 2003;60:405–14.
96. Tremblay F, Fernandes M, Habbab F, deB Edwardes MD, Loertscher R, Meterissian S. Malignancy after renal transplantation: incidence and role of type of immunosuppression. Ann Surg Oncol. 2002;9(8):785–8. PubMed PMID: 12374662.
97. Lutz J, Heemann U. Tumours after kidney transplantation. Curr Opin Urol. 2003;13(2):105–9. PubMed PMID: 12584469.
98. Végsö G, Toronyi E, Hajdu M, Piros L, Görög D, Deák PA, Doros A, Péter A, Langer RM. Renal cell carcinoma of the native kidney: a frequent tumor after kidney transplantation with favorable prognosis in case of early diagnosis. Transplant Proc. 2011;43(4):1261–3. PubMed PMID: 21620106.
99. Engels EA, Pfeiffer RM, Fraumeni Jr JF, Kasiske BL, Israni AK, Snyder JJ, Wolfe RA, Goodrich NP, Bayakly AR, Clarke CA, Copeland G, Finch JL, Fleissner ML, Goodman MT, Kahn A, Koch L, Lynch CF, Madeleine MM, Pawlish K, Rao C, Williams MA, Castenson D, Curry M, Parsons R, Fant G, Lin M. Spectrum of cancer risk among US solid organ transplant recipients. JAMA. 2011;306(17):1891–901.
100. Kasiske BL, Snyder JJ, Gilbertson DT, Wang C. Cancer after kidney transplantation in the United States. Am J Transplant. 2004;4(6):905–13. PubMed PMID: 15147424.
101. Szmidt J, Durlik M, Gałazka Z, Nazarewski S, Górnicka B, Ziarkiewicz-Wróblewska B, Bojakowski K, Nowacka-Cieciura E, Lao M. Low-stage renal carcinoma of the native kidneys in renal transplant recipients. Transplant Proc. 2002;34(2):583–4. PubMed PMID: 12009631.
102. Leveridge M, Musquera M, Evans A, Cardella C, Pei Y, Jewett M, Robinette M, Finelli A. Renal cell carcinoma in the native and allograft kidneys of renal transplant recipients. J Urol. 2011;186(1):219–23.
103. Klatte T, Marberger M. Renal cell carcinoma of native kidneys in renal transplant patients. Curr Opin Urol. 2011;21(5):376–9.
104. Prando A, Prando D, Prando P. Renal cell carcinoma: unusual imaging manifestations. Radiographics. 2006;26(1):233–44.
105. Israel GM, Silverman SG. The incidental renal mass. Radiol Clin North Am. 2011;49:369–83.
106. Gerst S, Hann LE, Li D, Gonen M, Tickoo S, Sohn MJ, Russo P. Evaluation of renal masses with contrast-enhanced ultrasound: initial experience. Am J Roentgenol. 2011;197(4):897–906.
107. Fan L, Lianfang D, Jinfang X, Yijin S, Ying W. Diagnostic efficacy of contrast-enhanced ultrasonography in solid renal parenchymal lesions with maximum diameters of 5 cm. J Ultrasound Med. 2008;27(6):875–85.
108. Vikram R, Ng CS, Tamboli P, Tannir NM, Jonasch E, Matin SF, Wood CG, Sandler CM. Papillary renal cell carcinoma: radiologic-pathologic correlation and spectrum of disease. Radiographics. 2009;29(3):741–54.
109. Cox J, Colli JL. Urothelial cancers after renal transplantation. Int Urol Nephrol. 2011;43(3):681–6.
110. Borhani AA, Hosseinzadeh K, Almusa O, Furlan A, Nalesnik M. Imaging of posttransplantation lymphoproliferative disorder after solid organ transplantation. Radiographics. 2009;29(4):981–1000.
111. Ali MG, Coakley FV, Hricak H, Bretan PN. Complex posttransplantation abnormalities of renal allografts: evaluation with MR imaging. Radiology. 1999;211(1):95–100. PubMed PMID: 10189458.
112. Lopez-Ben R, Smith JK, Kew 2nd CE, Kenney PJ, Julian BA, Robbin ML. Focal posttransplantation lymphoproliferative disorder at the renal allograft hilum. AJR Am J Roentgenol. 2000;175(5):1417–22. PubMed PMID: 11044055.